# Mineralogy and mixing state of North African mineral dust by on-line single-particle mass spectrometry.

Nicholas A. Marsden[1], Romy Ullrich[2], Ottmar Möhler[2], Stine Eriksen Hammer[3], Konrad Kandler[3], Zhiqiang Cui[4], Paul I. Williams[1,5], Michael J. Flynn[1], Dantong Liu[1], James D. Allan[1,5], and Hugh Coe[1]

[1]School of Earth and Environmental Sciences, University of Manchester, UK
[2]Institute of Meteorology and Climate Research, Karlsruhe Institute of Technology, Germany
[3]Institute of Applied Geosciences, Technische Universitat Darmstadt, Germany
[4]School of Earth and Environment, University of Leeds, UK
[5]National Centre for Atmospheric Science, Manchester, UK

*Correspondence to:* Hugh Coe (hugh.coe@manchester.ac.uk)

**Abstract.** The mineralogy and mixing state of dust particles originating from the African continent influences climate and marine ecosystems in the North Atlantic due to its effect on radiation, cloud properties and biogeochemical cycling. However, these processes are difficult to constrain because of large temporal and spatial variability, and the lack of in-situ measurements of dust properties at all stages of the dust cycle. This lack of measurements is in part due to the remoteness of potential source areas (PSA) and transport pathways, but also because of the lack of an efficient method to report the mineralogy and mixing state of single particles with a time resolution comparable to atmospheric processes, which may last a few hours or less. Measurements are equally challenging in laboratory simulations where dust particles need to be isolated and characterised in low numbers whilst conditions are dynamically controlled and monitored in real time. This is particularly important in controlled expansion cloud chambers (CECC) where ice nucleating properties of suspended dust samples are studied in cold and mixed phase cloud conditions.

In this work, the mineralogy and mixing state of the fine fraction ($< 2.5 \mu m$) in laboratory suspended dust from PSA in North Africa were made using novel techniques with on-line single-particle mass spectrometry (SPMS) and traditional off-line scanning electron microscopy (SEM). A regional difference in mineralogy was detected, with material sourced from Morocco contained a high number fraction of illite like particles in contrast to Sahelian material which contains potassium and sodium depleted clay minerals like kaolinite. Single-particle mixing state had a much greater local variation than mineralogy, particularly with respect to organic/biological content. Applying the same methods to ambient measurement of transported dust in the marine boundary layer at Cabo Verde in the remote North Atlantic enabled the number fractions of illite/smectite clay mineral (ISCM), non-ISCM, and calcium containing particles to be reported at a 1 hour time resolution over a 20 day period. Internal mixing of silicate particles with nitrate, chlorine and organic/biological material was also measured and compared to that in the suspended soils.

The results show SPMS and SEM techniques are complimentary and demonstrate that SPMS can provide a meaningful high-resolution measurement of single-particle mineralogy and mixing state in laboratory and ambient conditions. In most cases, the difference in mineralogy between particles within a soil sample was continuous, rather than a collection of particles with

discrete mineral phases. In ambient measurements, the ISCM and nitrate content was found to change significantly between distinct dust events, indicating a shift in source and transport pathways which may not be captured in off-line composition analysis or remote sensing techniques.

*Copyright statement.* TEXT

## 1 Introduction

Aeolian dust derived from sources in North Africa has a substantial impact on the climate and ecosystems in the North Atlantic but our ability to simulate climate response is poor (Evan et al., 2014; Kok et al., 2018). During aeolian transport, mineral dust influences many atmospheric processes, many of which are a function of mineralogy as well as particle size and elemental composition (Formenti et al., 2011). In addition, deposition of terrestrial material into the North Atlantic ocean is important to the biogeochemical cycle of marine ecosystems as it represents a major source of iron, nitrogen and phosphorous (Baker et al., 2003; Jickells et al., 2005).

In recent years, the composition of dust has attracted extra attention because mineral phase is thought to influence the ice nucleating (IN) ability of single particles (Zimmermann et al., 2008; Connolly et al., 2009; Möhler et al., 2008; Cziczo et al., 2009; Niedermeier et al., 2011; Augustin-Bauditz et al., 2016) and therefore influences climate by changing the radiative properties of ice and mixed phase clouds (Rosenfeld et al., 2001; DeMott, 2003), which represent some of the biggest uncertainties in weather and climate change prediction (DeMott et al., 2010; Carslaw et al., 2013). The mechanisms involved are not well understood and many analytical techniques have been developed to help further our understanding of this important single particle process (Hoose and Mohler, 2012; Hiranuma et al., 2015). Recently, it has been demonstrated that mineral phase has an influence on heterogeneous freezing temperature, with some feldspar group minerals proving to be particularly efficient ice nucleating particles (INP) in droplet freezing experiments with nominally pure laboratory prepared mineral samples (Atkinson et al., 2013; Harrison et al., 2016; Peckhaus et al., 2016).

To complicate things further, cloud chamber studies of silicate mineral dust coated with secondary sulphate and organics have demonstrated that this mixing can alter hygroscopicity and change the ice nucleation efficiency of a particle but is dependent on the ice forming mechanism (Möhler et al., 2008; Sullivan et al., 2010a, b; Niedermeier et al., 2011; Reitz et al., 2011). In addition, laboratory studies have suggested that the internal mixing state, particularly metal oxide - clay mineral assemblages, has important influence on direct radiative properties of dust (Nousiainen et al., 2009; Jeong and Nousiainen, 2014; Kemppinen et al., 2015; Di Biagio et al., 2017; Caponi et al., 2017). This highlights the need for measurement of single-particle composition, including both mineralogy and internal mixing state, but is extremely challenging in natural dust particles due to complex mineralogy and mixing state that is a product of the source area, emission mechanism, and atmospheric processing.

Major dust emission occurs in sparsely vegetated arid areas, but only when the surface properties and meteorological conditions are favorable (Knippertz and Todd, 2012), which can be difficult to predict in dust emission models (Heinold et al.,

2013). During the summer months in North Africa, the process of dust advection is associated with moist convection (Schepanski et al., 2009b) and results in a complex structure of stratified layers of warm dry air with very high dust concentrations (Dunion and Marron, 2008). Satellite observations show that these layers can be transported westward in discrete plumes over the Atlantic Ocean towards the Caribbean basin (Kaufman et al., 2005; Zhu et al., 2007; Doherty et al., 2008; Tsamalis et al., 2013).

The source of these dust plumes are arid soils that consist of a complex mixture of organic and inorganic material. The inorganic material largely consists of silicate minerals (quartz, feldspars, clay minerals), carbonate and metal oxides that occur as whole grains or mixed mineral phases. The abundance of mineral phase has a strong grain size dependence, with quartz occurring in the coarse fraction and clay minerals dominating the fine fraction, but the size distribution is modified during emission (Perlwitz et al., 2015a), so that ratios of mineral phases in the lofted mineral dust aerosol may not be completely representative of that of the source soil. Aircraft observations have demonstrated that the size distribution of dust plumes also evolve during transport which affects optical properties (Ryder et al., 2013), but the contribution from associated changes in composition are not understood.

Measurements of ambient dust properties are needed to inform simulations of dust emission, transport and deposition processes in present day climate and paleoclimate models. For example, the provenance of mineral dust has been determined by comparing mass fraction ratios of certain mineral phases to the bulk analysis of soils in potential source areas (PSA) (Caquineau et al., 2002; Scheuvens et al., 2013). Although improved soil maps are available for North Africa (Claquin et al., 1999; Nickovic et al., 2012; Journet et al., 2014), they still lack the spatial resolution required to represent the heterogeneity of soil within a PSA and results in an over simplification of the mineralogical relationships in a given soil type (Scanza et al., 2015). Improvements to emission simulations require validation measurements of size resolved dust mineralogy and mixing state at varying distances from the source (Perlwitz et al., 2015b).

Identification of the source of transported dust is problematic due to the inhomogeneity of source sediments and the mixing of material during transport. Nevertheless, analysis of bulk mineralogical composition of source sediments can provide markers, with illite/kaolinite ratios being particularly useful (Caquineau et al., 2002). At the Cabo Verde Islands, Glaccum and Prospero (1980) analysed day long exposures of filters during the summer of 1974 and concluded that illite and mica were the dominant mineral types deposited in the tropical North Atlantic. In contrast, Kandler et al. (2011a) reported kaolinite as the dominant mineral type and attributed this to the dominance of sources in the Sahel during the summer.

Silicates are the most important group of rock-forming minerals and comprise a huge spectrum of compositions and crystal structures. However, the fine fraction of continental soil largely consists of clay minerals with minor amounts of feldspar and quartz (Perlwitz et al., 2015b). Clay minerals are phyllosilicates which consists of 2D layers of silicon tetrahedrally co-ordinated with oxygen, and aluminum octohedrally co-ordinated with oxygen and/or hydroxyl. A simple example is that of the mineral kaolinite $\left(Al_2Si_2O_5(OH_4)\right)$, in which these two layer types are repeated to form a 3D structure referred to as 1:1 layer structure (Fig. 1(a)).

A more complicated structure results in the presence of large cations of potassium, sodium and calcium. The charge and ionic radius if these cations is accommodated in a separate sheet of interstitial cations that must be charged balanced by the

tetrahedral and octohedral layers. In the case of potassium, charge balance is achieved with the common 2:1 layer structure of illite $\left(K_{1.5-1.0}Al_4[Si_{6.5-7.0}Al_{1.5-1.0}O_{20}](OH_4)\right)$ in which there are two tetrahedral layers for each octohedral layer (Fig. 1(b)). These types of clay mineral are expected to be abundant in Saharan dust. For example, in a previous study using transmission electron microscopy (TEM) of sliced dust particles collected at the island of Tenerife in the North Atlantic, the majority

5  of particles of transported Saharan dust were clay rich agglomerates primarily composed of a matrix of illite/smectite clay minerals (ISCM) with inclusion of kaolinite and hematite (Jeong et al., 2016).

The feldspar group of minerals are chemically similar to the clay minerals but a higher atomic content of alkali and alkaline earth metals demands a different crystal structure to achieve charge balance. In K-feldspars $\left(K[AlSi_3O_8]\right)$, such as microcline and orthoclase, interstitial cations of potassium are fixed in a cavity where they are charge balanced by a 3D network of

10  tetrahedrally co-ordinated silicon and aluminum (Fig. 1(c)). Whilst these minerals are expected to be less common than clay minerals in fine mineral dust, they may be particularly important in ice nucleation in the atmosphere.

The analytical challenge arises from the fact that common mineral phases are very similar in composition, and undergo significant alteration and weathering in the soil making pure minerals difficult to identify (Formenti et al., 2014). For example, in clay minerals, potassium, sodium and calcium are interchangeable during the weathering process so that composition is not

15  necessary uniform throughout the crystal lattice. Indeed, the illite structure in Fig. 1(b) is the idealised version of the pure mineral, which is often referred to as an end-member of the illite series. Complete uniformity of clay mineral composition is unlikely on the scale of a single particle or between particles from the same soil sample.

In order to identify the mineral phases present, one must either make an accurate quantitative measurement of the elemental composition or make an analysis of crystal structure. An established approach to both ambient and laboratory measure-

20  ments is to collect particles on filters and impactors for subsequent off-line analysis. Bulk mineralogy can be obtained with crystal structure analysis by X-ray diffraction (XRD), and the composition of individual particles is assessed by advanced microscopy. Scanning Electron Microscopy (SEM), often combined with energy-dispersive X-ray spectrometry (EDX), is a powerful method for elucidating composition because of the ability to probe the composition of individual dust particles. The application of these techniques can differentiate silicate from calcium rich particles and show evidence of heterogeneous

25  reactions in the atmosphere (Ro et al., 2005; Jeong and Chun, 2006; Sobanska et al., 2012).

However, further differentiation of silicate mineral phase in single particles is hampered by the difficulty in leveraging the full quantitative capability of SEM due to particle morphology effects. Consequently, silicate particles are often reported in compositional groups, which describes the dominant elemental features but not actual mineral phase (Kandler et al., 2009; Hammer et al., 2018). In addition, there are a number of drawbacks to this off-line approach including; labor intensive post

30  sampling analysis, and loss of temporal resolution in dynamic situations.

A second, but less common approach is to use single-particle mass spectrometry (SPMS) to provide an on-line assessment of aerosol composition. An advantage is that the high temporal resolution allows the evolution of the particle composition to be measured in a dynamic setting (Cziczo et al., 2006; Zelenyuk et al., 2009; Gaston et al., 2013), and the instruments can be deployed in-line with other techniques such as counterflow virtual impactor (CVI) to measure ice residuals (Cziczo et al., 2003;

35  Gallavardin et al., 2008; Baustian et al., 2012; Zelenyuk et al., 2015; Worringen et al., 2015; Schmidt et al., 2017). However,

compositional analysis with SPMS is fraught with difficulties relating to poor reproducibility, and the non-quantitative nature of the measurement associated with instrument function and particle matrix effects (Reilly et al., 2000; Sullivan and Prather, 2005; Murphy, 2007; Hatch et al., 2014).

The matrix effects arise from the incomplete desorption and ionisation process and the subsequent competitive ionisation of atoms and molecular fragments, so that co-variance of analyte signals is relative to ionisation energy and electron affinity of the surrounding matrix (Reinard and Johnston, 2008). In circumstances where the composition of the matrix is known a priori, careful calibration with a suitable proxy can produce quantitative or semi-quantitative measurements of an analyte within a single particle (Gross et al., 2000; Bhave et al., 2002). However, if the particle matrix is complex, such as in soils and transported dust, this type of calibration cannot be made due to the lack of a suitable proxy.

Despite these limitations, SPMS can characterise a particle population by classifying particle types and measuring temporal trends in particle number concentrations using cluster analysis (Hinz et al., 2006; Rebotier and Prather, 2007; Gross et al., 2010). Although the reported number concentration are also not fully quantitative (Murphy, 2007), a relative trend in certain particle types can be achieved. This techniques have been used to discriminate mineral dust particles from other refractory aerosol types such as sea salt (Sullivan et al., 2007a; Dall'Osto et al., 2010; Fitzgerald et al., 2015; Schmidt et al., 2017), but cannot differentiate the actual mineral phase of silicates within dust particles. More recently, a machine learning technique has shown promise with the classification of mineral dusts of similar composition (Christopoulos et al., 2018), but this techniques also requires suitable mineral dust proxies for training data.

In a previous study using a single particle mass spectrometer (LAAPTOF, AeroMegt GmbH), Marsden et al. (2018) presented a novel method for the assessment of single crystal structure that, when used in tandem with the more typical elemental composition measurement, performed an on-line differentiation of single particles of kaolinite, illite and K-feldspar mineral phases. In the present study, we applied a refined version of these techniques to suspended natural soils sampled at the Aerosol Interactions and Dynamics in the Atmosphere (AIDA) facility at the Karlsruhe Institute of Technology (KIT), as part of the ice nucleation research unit (INUIT) program studying heterogeneous ice formation in the atmosphere (https://www.ice-nuclei.de/the-inuit-project/). The results of analysing soil from PSAs in North Africa were used to interpret ground based ambient measurements of transported dust at Praia, Cabo Verde in the tropical North Atlantic during the summer of 2015 as part of the Ice in Clouds Experiment- Dust (ICE-D) campaign.

## 2  Methods

A limited number of mineral phases were chosen to create fingerprints to which the more varied mineralogy of naturally occurring sediments could be compared. Nominally pure samples of illite, Na-montmorillonite, kaolinite; along with ortho-clase (K-feldspar), plagioclase (Na-feldspar) were used to represent the end members of the clay minerals and feldspar groups respectively, based on the assumption that the fine fraction ($< 2.5 \mu m$) continental sediment is primarily composed of alumi-nosilicate clays and feldspars. Quartz and carbonate minerals are not considered with sub-compositional analysis due to the inability of the LAAPTOF to efficiently ablate pure quartz and the apparent lack of a clear carbonate signal respectively. In

ambient dust, calcium rich particles are considered separately to aluminosilicate particles after being separated using traditional cluster analysis techniques.

The LAAPTOF instrument and data analysis methods are described below, along with SEM-EDX methods used to obtain elemental composition of the laboratory suspended dust for method validation. The experimental setup of the INUIT09 laboratory campaign and ICE-D ambient measurement are also described in this method section.

## 2.1 LAAPTOF Single particle mass spectrometry

In a previous study, Shen et al. (2018) showed that the LAAPTOF single particle mass spectrometer is capable of distinguishing the composition of different particles in the ambient environment using a combination of fuzzy clustering and reference based spectra classification, whilst Ahern et al. (2016) demonstrated a positive correlation between ion signals of organic markers and the quantity of condensed organic coating, despite inhomogeneity in the soot core of the particles. These studies show that the LAAPTOF is an appropriate platform for studying the composition and internal mixing state of refractory aerosol.

In SPMS, aerosol is directly introduced into the instrument via a pumped inlet so that sample collection and preparation are not required. Particle composition is analysed by time-of-flight mass spectrometry (TOFMS) after laser desorption ionisation (LDI) of individual particles using a high powered UV laser. The LAAPTOF instrument features an aerodynamic lens inlet, optical particle detection, LDI ion source and bipolar TOFMS as previously described by Gemayel et al. (2016). Within the instrument, LDI is performed by ArF excimer laser (model EX5, GAM Laser Inc.), set to deliver 3-5mJ/pulse of 193nm radiation with a pulse width of 8ns.

Like all single particle mass spectrometers, the LAAPTOF measurements is subject to a number of biases that result in preferential transmission, detection and ablation efficiencies of certain particles (Murphy, 2007). The instrument used in this investigation features a modified particle detection system based on a fibre-coupled laser delivery that allows the simple interchange of laser systems of different wavelengths. The instrument is capable of providing size resolved composition measurements for up to 200 particles per second in the size range approx. $0.4 - 2.5 \mu m$, but the actual detection efficiency of particles within this range depends on the size, shape and composition, as well as the wavelength of the optical detection system. Differences in instrument setup between the laboratory and ambient measurements that may impact the comparison of the two data sets are presented in Supplement S1.

Laboratory evaluation of the fiber-coupled laser system indicated that the peak detection efficiency is 0.25 with spherical particles Marsden et al. (2016), but the overall efficiency of the instrument also depends on ablation efficiency with respect to particle composition. In a study of nominally pure mineral samples, Marsden et al. (2018) reported the number of optically detected particles that produced a mass spectra (i.e. ablation efficiency or hit rate) of 0.29 and 0.14 for illite and kaolinite respectively, but was also dependent on the amount of impurities such as Titanium. Furthermore, from the authors own experience, it likely that pure quartz may have an ablation efficiency close to zero and is not considered in our analysis, but is unlikely to be a major component in the fine fraction in any case. The potential maximum overall efficiency (detection efficiency * ablation efficiency) of the LAAPTOF measurement of clay mineral ranges from 0.0725 for pure spherical particles particles of

illite, to 0.035 for pure spherical particles of kaolinite. The exact efficiency of the instrument is not known in most situations because the size, shape and composition of the particles would have to be known a priori for accurate calibration.

### 2.1.1 Crystal structure analysis of silicates

In a study of ion formation mechanism, Marsden et al. (2018) showed that the ionisation potential and co-ordination of interstitial cations has a strong influence on how the crystal structure breaks apart during LDI process of silicate particles. This is exploited for the differentiation of mineral phase by the measurement of average ion arrival of the $O^-$ and $SiO_3^-$ ion species, which is thought to record the initial kinetic energy of the ionic fragments during ablation.

With this technique we can compare the structure of soil dust samples to nominally pure mineral samples on a particle by particle basis. Laboratory calibrations have demonstrated that for ISCM the abundance of exchangeable sodium and potassium cations results in a unique range of $\tau$ values between 0.2-0.58. Feldspars typically produce $\tau$ values >0.58 (Fig. 2) due to the interlocking nature of the interstitial cation in their crystal structure. Kaolinite and amorphous glass produces $\tau$ values close to 1 due to the complete absence of interstitial cations and lack of crystal structure respectively.

### 2.1.2 Sub-compositional analysis of silicates

Sub-compositional analysis is a technique that is commonly used for the analysis of complex chemical relationships in circumstances in which the full composition of a substance is impossible to obtain, such as in whole-rock geochemical analysis (Pawlowsky-Glahn and Egozcue, 2006), where it is convenient to describe the composition in terms of a relative measurement of carefully chosen components. The ternary diagram provides an intuitive way of displaying relative information whilst avoiding some of the sub-compositional incoherence associated with two component systems. The technique has been applied to the single particle analysis of natural Asian mineral dust using SEM (Yuan et al., 2004), and transported Asian dust using SPMS (Sullivan et al., 2007a). It is particularly well suited to SPMS because the composition obtained from the mass spectra is inherently sub-compositional due to the matrix effect.

Sub-compositional analysis was used to produce fingerprints of pure mineral phases using the ternary system $Al^+ + Si^+, K^+, Na^+$, cations readily observed in the SPMS of mineral dust (m/z 27, 28, 39, 23 respectively). Source clay material from the clay mineral society and crushed feldspar crystals were suspended in a home made dust tower in the experiment described in Marsden et al. (2018). Elemental composition and mineralogy of these samples have been previously characterised and can therefore be used as reference fingerprints for comparison with natural soil. Ternary diagrams of the clay minerals and feldspar standards are displayed separately in Fig. 3.

The 2D space in these diagrams are non-linear and due to the matrix effect, a fully quantitative composition cannot be deduced from these plots alone, but it is interesting to note that K-feldspar appears less K and Na rich than illite clay despite the structural formula and X-ray flourescence analysis of the bulk sample indicating the contrary. This is because the tetrahedral framework of the feldspar makes the release of interstitial $K^+$ and $Na^+$ without also releasing $Al^+$ improbable, whereas they can be released independently of $Al^+$ from the weakly bonded interlayer in 2:1 clay structure.

Although the elemental sub-composition measurement is clearly non-quantitative with respect to bulk XRF analysis, the measurement is semi-quantitative (relative) with respect to samples of minerals with the same crystal structure. For example, a clear separation between K and Na rich feldspar is apparent in Fig. 3, which is relative to their actual elemental ratios. This is not true if comparing the clay mineral illite with the framework silicate K-feldspar, which would not be easily distinguishable from each other if plotted in the same space, despite the clear differences in elemental composition. It is therefore necessary to apply crystal structure analysis to achieve semi-quantitative composition and distinguish clay minerals from feldspar when analysing natural soils with SPMS.

### 2.1.3 Sub-composition analysis of internal mixing state

Internal mixing of non-mineral species can occur during soil formation or during transport in the atmosphere where heterogeneous reactions take place on the surface of the particle (Usher et al., 2003). Reactions with nitric, sulphuric and organic acids can produce nitrate, sulphate and organics on the particle surface respectively. Reference spectra obtained with the LAAPTOF during the FIN-1 campaign show the presence of sulphate marker $HSO_4(m/z97)$ on particles after mixing suspended feldspar with ozone and sulphuric acid in the AIDA chamber (Fig. 4(b)). Similarly, organic markers $C_2, C_2H$ and $C_2H_2(m/z24, 25, 26)$ appear on particles after mixing suspended feldspar with ozone and $\alpha$-pinene (Fig. 4(c)). Only small organic fragments are observed due to the extensive fragmentation of organic molecules. These ion combinations have also been observed on ambient mineral dust using SPMS instruments (Silva and Prather, 2000; Sullivan et al., 2007a; Fitzgerald et al., 2015).

In ambient dust, organic or biological material may have been mixed with a dust particle in the soil before emission. Indeed, the transport of microorganisms in dust storms is human health concern (Griffin, 2007). Recently, Yamaguchi et al. (2012) provided direct evidence of bacterial cells on Asian dust particles and demonstrated a global dispersion pathway through dust transport. The internal mixing of biological material with dust particles is therefore of interest. LAAPTOF reference spectra of bacteria, also from the FIN-1 campaign, show strong signals of $CN$ and $CNO(m/z26, 42)$ (Fig. 4(d)) representing fragments of nitrogen containing organic compounds. These markers have been attributed to compounds of biological origin (Pratt et al., 2009; Cahill et al., 2012; Creamean et al., 2013), although other studies have found these markers in aerosol where biological components were not expected (Sodeman et al., 2005; Zawadowicz et al., 2017; Wonaschuetz et al., 2017). Consequently, we describe these markers as organic-biological (Org-Bio hereafter).

Internal mixing of natural soil samples with non-minerals in this work are considered with the ternary sub-composition $Cl^-, CN^- + CNO^-, SO_4^-$. These markers represent compounds that could be present in soils and ambient dust, but are not present in silicate minerals structure. Phosphate marker $PO_3^-$ is not considered because it could be derived from the calcium phosphate mineral apatite as well as biological material, and it therefore not a reliable indicator of mixing state. The $Cl^-$ elemental ion is included despite it also having mixed provenance such as primary chlorides or secondary uptake of $HCl$ (Sullivan et al., 2007b), because it is preferentially ionised due to very high electron affinity and therefore is included as a reference that would otherwise perturb the measurement. It is also an indication of the purity of silicate particles as pure fresh silicate should not contain Chlorine.

## 2.2 Scanning electron microscopy

Particles were sampled from the AIDA chamber with a single-stage nozzle impactor ($50\%$ low cut-off diameter at approximately $0.1\mu m$ aerodynamic diameter; for specifications see Kandler et al. (2007)) on nickel grids (TEM grids type S162N9, Plano, Wetzlar, Germany). The inlet was connected to a sampling line on the AIDA chamber and the sample time varied between 12-16 min.

All samples were analysed with computer controlled scanning electron microscopy (ccSEM) using a FEI Quanta 400 FEG instrument (FEI, Eindhoven, The Netherlands) equipped with an energy-dispersive X-ray detector, X-Max150 (Oxford, Oxfordshire, United Kingdom), and the Oxford software Aztec (version 3.3 SP1). An acceleration voltage of 12.5 keV, spot size 5, a working distance of 10mm and high vacuum conditions ( $10^{-5}hPa$) were used for all samples. Backscatter electron images were used to segment particles from substrate. The particles of interest were measured with 4 seconds counting time for X-ray microanalysis. The TEM grids were mounted in a copper sample holder (avoiding interference with chemical composition of the particle) equipped with a beam trap (maximizing the characteristic-peak-to-background ratio).

Chemical composition of all elements with atomic number higher than 3 (Li) was determined with energy-dispersive X-ray microanalysis. A sorting step after ccSEM was performed to remove particles with low X-ray counts (due to shading effects) and features of the TEM grid. Between 159 and 776 alumosilicates were detected per samples with the highest abundance of particles at an average diameter of $200nm$.

The traditional method for reporting the composition of aerosol particles involves the classification of particles into compositional groups using a variety of elemental ratios and boundary rules e.g Kandler et al. (2007, 2011b); Young et al. (2016). However, these classification systems are impossible to apply to SPMS due the matrix effects that skews and suppresses elemental ratios. We therefore choose to display the SEM composition as ratios of Al/Si, (K + Na)/Si and (Fe + Mg)/Si ratios, which leverages the quantitative ability to produce a representation of the interstitial cation and aluminosilicate structure that can be intuitively compared to the ternary diagrams obtained by SPMS.

Scatterplot of single particle average chemical composition is plotted in Fig. 5(a). This demonstrates that pure mineral can potentially be differentiated using quantitative $Al/Si$ ratio and the $(K+Na)/Si$ (cation to silicate) ratio. For example, the pure Kaolinite clay mineral has the highest $Al/Si$ ratios ($\approx 1$) but no $(K+Na)$ content. In general, the decreasing $Al/Si$ ratio must be balanced by increasing cation/Si ratio in clay minerals.

## 2.3 INUIT09 Laboratory Suspended Dust Experiment

### 2.3.1 Experiment Setup

For the aerosol generation during the INUIT09 campaign, the natural dust samples were sieved to diameters less than $75\mu m$ and injected in either the AIDA cloud chamber or the Aerosol Preparation and Characterisation (APC) chamber. For injection, a rotating brush generator linked to a cyclone impactor was used, resulting in aerosol particles with aerodynamic diameters of less than about $5\mu m$. The dust number concentration in the AIDA chamber was initially between 200 and $300cm^{-3}$ and in

**Table 1.** Sampling location of natural soils for laboratory experiments

| Sample | Location | Notes |
|---|---|---|
| DDS01 | 29.83773 °N, -5.76143 °E | River sediments |
| DDS02 | 29.84957 °N, -6.01508 °E | Hamada with large amounts of dust |
| DDS03 | 29.86202 °N, -6.156760°E | Border of dry salt/ silt plain |
| SDN02 | 13.516667 °N, 2.633333 °E | Banizoumbou, Niger |
| SDN05 | 13.522203 °N, 2.133011 °E | Grand Mosque, Niamey, Niger |
| DDA01 | | Dano, Burkina Faso |

*Signal line attenuation changes the saturation and limit of detection of the ion detection system

the APC chamber between $1000$ and $5000 cm^{-3}$. The number concentrations and size distribution of the dispersed aerosol are detailed in Supplement S2.

During this study, the single particle mass spectrometer LAAPTOF was either connected to the AIDA chamber or the APC, and sampled for about 1 hour during each experiment. During the sampling time, both the AIDA chamber and APC chamber were held to nearly constant temperature (either $-16 \deg C$ or $-21 \deg C$ in AIDA and $25 - 27 \deg C$ in APC) and pressure ($998 - 1010 hPa$ in AIDA and $990 - 1005 hPa$ in APC chamber) conditions.

### 2.3.2 Soil Sampling Locations

Soil samples from two specific ecoclimatic zones were suspended at the AIDA facility; the mountainous north-west margin of the Sahara Desert, and the west-central Sahel beyond the southern margin of the Sahara Desert (here-after named Sahel Dust). These PSA were chosen because there is likely to be differences in mineralogical composition between the two zones. Analysis of surface material across North Africa are scarce, but the available studies demonstrate a North-South decease in illite/kaolinite (I/K) ratio in the clay fraction (Caquineau et al., 2002; Scheuvens et al., 2013; Formenti et al., 2014) mainly due to differences in diagenetic history between dry and wet climate zones.

The sampling locations of the natural arid soils are displayed in Fig. 6. Moroccan dust samples were collected in the Mhamid region, on the upper Draa valley, Morocco during the Saharan mineral dust experiment (SAMUM) (Ansmann et al., 2011). The Draa valley is a large geographical feature on the Southern edge of the Anti-Atlas mountains, beyond which is the Sahara desert of Algeria. All sampling locations fall within unit 1336 in Digital Soil Map of the World (DSMW), compiled by the Food and Agriculture Organization (FAO) of the United Nations (FAO, 1995, 2007).

The samples of Sahel soil were collected from diverse geographical locations in Niger and Burkina Faso. All three sampling locations fall within the zone of kaolinite rich soil (Fig. 6) where the DSMW indicates cation exchange capacity (CEC) <35 cmol/kg.

## 2.4 Ambient Measurement at Cabo Verde during ICE-D

The Cabo Verde archipelago is a favorable location for remote marine measurements. Situated some 800km off the West coast of North Africa (Fig. 6), it is a site at which long term measurements of greenhouse gasses, trace gasses and aerosol properties are recorded (Carpenter et al., 2010). Notable studies of mineral dust composition in the area include long term filter sample collection at Cape Verde atmospheric observatory (CVAO) (Patey et al., 2015) and Praia City, Santiago Island (Salvador et al., 2016), and filter collection at Praia Airport, Santiago Island for the SAMUM campaign January-February 2008 (Kandler et al., 2011a).

Ground based ambient measurements during ICE-D took place in the mobile Manchester Aerosol Laboratory located within the perimeter of Praia International Airport, Santiago Island, Cabo Verde, (14°57'N 23°29' W, 100 m asl), approximately 1500m from the coast and 150m from the airport runway. The main airport terminal and the outskirts of the city of Praia were 400m and 2500m downwind of the prevailing NE wind respectively. Aerosol was sampled via a 6 inch plastic inlet fixed to a 10m tower and pumped at 185l/min. The flow was distributed to a suite of on-line instruments, including the LAAPTOF, via a system of 48mm ID lines isokinetically sampled from the main inlet, and heated to 19°C.

## 3 Results and Discussion

### 3.1 Single particle analysis of laboratory suspended natural soil (INUIT09)

The sampling of particles took place after dispersing the source material in the APC chamber using a rotating brush generator. The resulting particle concentration and size distribution is dynamic but is typically on the order of $1000cm^{-3}$ with a particle size mode at $200nm$ (See supplement S2), which is below the lower size cut of the LAAPTOF, but not the filter collection. Although the two measurement techniques are not performed on the exact same particle sizes. Still, both measurements represent the fine fraction ($< 2.5\mu m$) of the dispersed dust.

#### 3.1.1 Silicate mineralogy of laboratory suspended soil (INUIT09)

SEM EDX analysis of the suspended soil shows that the composition of single particles within each soil type varies in a continuous distribution rather than in distinct clusters (Fig. 5). A distinct difference in the elemental composition of soil from the Northern Sahara and the Sahel exists in these diagrams, particularly with respect to the Al/Si ratio. The Moroccan soils (Fig. 5(b-c)) have a spread in compositions close to the illite plotted on the diagram, with the DDS01 samples being more diverse than the DDS02. In contrast, the soil from the Sahel (Fig.5(c-f)) consists of material with higher Al/Si ratio which approaches the composition of the plotted kaolinite. This is in agreement with CEC measurements of sediment in PSA which show that kaolinite fraction in soils increases in soils in the Southern Sahel regions compared to the northern regions of the Sahara (Scheuvens et al., 2013).

SPMS mineralogical analysis proceeds by considering the relative abundance between $K$, $Na$ and $Al + Si$, which together define the phase of many minerals in the continental crust. This sub-compositional analysis was previously applied to nomi-

nally pure mineral samples from the clay mineral society (CMS) to provide a fingerprint reference for the common clay mineral phases (Fig. 7(a)). The same analysis applied to Moroccan dust (Fig. 7(a-c)) and Sahelian dust (Fig. 7(e-g)) shows key differences between the composition of the two ecoclimatic zones, with Moroccan dust tending towards an illite composition and Sahelian dust tending to a kaolinite composition, in agreement with the SEM EDX analysis.

5    Application of the crystal structure analysis (color function in Fig. 7) to each particle indicates that the majority of the particles are of a 2:1 clay structure, even in Sahelian dust particles that have a kaolinite (1:1 clay structure) like composition. This may suggest an impure kaolinite or montmorillonite that is not captured in the cation sub-composition due to the relatively high sensitivity to $K^+$ in the LAAPTOF measurement. A comparison of the sub-composition (Al+Si)/(Al+Si+K+Na) obtained by SPMS and SEM measurement (Fig. 8) demonstrates a much greater sensitivity to alkali metals in the SPMS measurement (due

10    to low ionisation energy) than in the established filter technique. The SEM techniques show a lower (Al+Si)/(Al+Si+K+Na) ratio in the Moroccan sample (DDS01, panel (a)) compared to the Sahel sample (SDN02, panel (c)), but this is greatly exaggerated in the SPMS analysis (panels (b) and (d)) due selective ionisation of K and Na and the matrix effect.

    In general, our analysis suggests the fine fraction of these North African soil samples to consist of $K$ rich and $Al$ rich clay minerals. This agrees somewhat with a comprehensive study of soil samples using many techniques by Engelbrecht

15    et al. (2016) that concluded suspended mineral dust particle were primarily made up of two types of mineral assemblages; i) fragments of micas, clays, oxides, and ions of potassium ($K^+$), calcium ($Ca^+$), and sodium ($Na^+$) rich colliods in amorphous clay-like material, and ii) kaolinite with individual oxide mineral grains. The exception is that our measurements indicate that the potassium and sodium are retained in a 2:1 clay structure rather than in amorphous clay.

    In order to explore the composition of potentially amorphous and feldspar matrix, we extracted particles with $\tau$ values of 0.58

20    - 0.8 into separate plots (Fig. 9). Perhaps unsurprisingly, the composition of these types of particles reflects the composition of clay particles (Fig. 7), with samples from the Sahel showing a greater loss of alkali metals due to weathering and diagenesis. It is not possible to separate felsic and amorphous material with any confidence, but it is reasonable to say that any feldspars that may be present in the Moroccan samples are fresher (un-altered) than their counterparts from the Sahel due to the higher potassium content. It is known that K-feldspar is progressively altered to quartz and kaolinite if the potassium is removed by

25    dissolution in the soil over .

    The sample that has potentially the most feldspar grains is DDS01 which shows a small number of particles with a felsic composition in the SEM EDX analysis (Fig. 5(b)), and maybe a reflection of the river sediment containing freshly eroded rock from the Anti-Atlas mountain range. This sample also displays a distinct mode in the SPMS $\tau$ histogram in the felsic/amorphous region (Fig. 7(d)). In general, the SPMS crystal structure analysis in the $\tau$ histograms agree with the SEM EDX analysis of the

30    distribution of composition in the samples. For example, the $\tau$ histogram of DDS02 indicates a predominately illite composition which is also reported in the narrow composition distribution in the SEM EDX analysis.

### 3.1.2   Internal mixing state of suspended natural soil

Unlike the mineralogical composition, the mixing state of the natural soil samples varies quite a lot within the same PSA (Fig. 10). All samples contain particles with significant amounts of chlorine. Sample DDS03, collected close to a salt/silt plain,

shows a relatively high sulfate content, probably associated with evaporite deposits. The biggest difference however is the relative amount of org-bio internally mixed in the particles. This is further demonstrated in the histograms of the normalised org-bio content displayed in Fig. 11. Most samples contain particles with significantly less org-bio than chlorine, but samples DDS01 and SDN02, collected from a dry river bed and agricultural land respectively, have a number of particles where the org-bio signal is even stronger than that of chlorine, which is significant given the high electron affinity of the later.

## 3.2  The composition and transport history of transported dust (ICE-D)

In order to examine the properties of the transported dust in the ambient measurement, the mass spectra of silicate particles must be extracted from the general aerosol population. This was achieved using the fuzzy c-means clustering supplied with the data analysis software (LAAPTOF Data Analysis v1.0.2). The analysis was performed on positive and negative ion spectra and on negative ion spectra only. In both cases, silicate and calcium classes of particles were reported along with sulphate, carbonaceous and abundant sea-salt particles. Analysis using only negative ion spectra proved more useful in the evaluation of mixing state because it was not subject to false class divisions caused by greater peak position shifting in positive ion spectra. A full description of the clustering analysis, including mass spectra of the cluster centers, is provided in supplement S3.

Averaged detection rate of the silicate and calcium particle types, as determined by the fuzzy clustering analysis, is displayed in Fig.12(a) with a 1 hour resolution . A previous comparison with an aerodynamic particle sizer indicated that the silicate particle count represented approximately $1\%$ of the actual silicate present due to instrument function (Marsden et al., 2016). Nevertheless, the temporal evolution of the particle classes is representative and compares well to the the dust fraction of incandescent particles identified in tandem Soot photometer (SP2) measurement (Liu et al., 2018).

### 3.2.1  Calcium rich particles

Calcium carbonate ($CaCO_3$) is the most abundant non-silicate material in arid soils and is expected to be a major constituent in mineral dust aerosol. However, pure calcium carbonate particles were not observed in this ambient measurement. Alkaline calcium carbonate particles are expected to readily react with acid gasses in atmosphere to form calcium salts. The reaction of calcium carbonate with nitric acid has been offered as a mechanism to explain $Ca(NO_3)_2$ on filters exposed to dusty environments (Krueger et al., 2004; Laskin et al., 2005; Matsuki et al., 2005; Hwang and Ro, 2006; Sobanska et al., 2012) collected after transport through urban and industrial areas. More recently, it has been suggested that in remote marine environments, a prevalence of $HCl$ over $HNO_3$ would favor the formation of $CaCl_2$ as the principal calcium salt (Tobo et al., 2009; Kim and Park, 2012).

A distinct calcium chloride particle class is reported in this ambient measurement. These particles are characterised by signals of $Ca^+(m/z 40)$, $CaO^+(m/z 56)$ and $CaCl^+(m/z 75, 77)$ in positive ion spectra and $Cl^-(m/z-35,-37)$, and $CaCl_3^-(m/z 145, 147, 149)$ in negative ion spectra (See supplement S3.2). The temporal evolution of this particle class is similar to that of the silicate particle class (Fig. 12(a)), but very different to that of the sea-spray particles (see supplement S3.5), therefore we conclude that is has a similar source to the silicate and probably represents calcium carbonate that has been processed in the atmosphere .

### 3.2.2 Temporal evolution of the silicate particle mineralogy (ICE-D)

In order to create a concise time series of the single particle mineralogy for the entire time period, the silicate class of particles (previously identified by cluster analysis) was differentiated into a simple binary system of ISCM and non-ISCM using the crystal structure analysis ($\tau$ parameter) to produce an time series of ISCM ratio (Fig. 12(b)). The ISCM ratio is the number of particles which have $\tau < 0.58$ divided by the number of silicate particles which have $\tau > 0.58$, representing ISCM and non-ISCM (feldspar, amorphous and pure kaolinite) respectively (See section 2.1.1). The average detection rate of silicate and calcium containing particles were combined to produce an hourly average of the ISCM, non-ISCM and calcium number fractions in mineral dust (Fig. 12(c)). Note that these fractions are relative to the detection efficiency of the instrument to each particle type, but the temporal evolution is representative.

Most of the measurement period was characterized by relatively high ISCM ratio which is generally »1. This is consistent with continuous long term off-line measurements of elemental composition around Cabo Verde by Patey et al. (2015) who concluded that illite was the most abundant clay mineral type. However, these conditions changed 17th August when the ISCM ratio is much lower than in the previous period with (ISCM ratio <1) and the fraction of calcium containing particle increases. We used the time series to define two dust events (D1 centered on 00:00 11/08/2015 and D2 centered on 15:00 17/08/2018) which were analysed in more detail with sub-compositional analysis, using the same method applied to the soil dust samples.

Silicate dust in event D1 contained a high fraction of ISCM type mineral composition with 2:1 phyllosilicate structure (blue circles in Fig. 13(a)), that plot close to the illite composition in the ternary diagram, similar to that observed in Moroccan soil DDS01 and DDS02 (Fig. 7(b, c)), In contrast, these ISCM particles is much reduced in dust event D2 which has a higher proportion of non-ISCM (felsic or amorphous material (red circles in Fig. 13(e)), and a shift away from the illite composition on the diagram. The actual mineral phase of these particles is less clear, but from the large fraction of these particle types and there central position on the ternary diagram it would be reasonable to assume an mixed amorphous matrix. It is clear however that the large fraction of particles with illite matrix present in D1 are absent in D2. The potential source and transport history of these material in these dust events is discussed in more detail after consideratin of the mixing state below.

### 3.3 Temporal evolution of the mixing state of silicate particles (ICE-D)

The mixing of silicate and non-silicate within single particles may result from processes within the native soil (primary), or during atmospheric transport (secondary). The analysis of the suspended soil dust (INUIT09) shows mineral particles in North African soils are already mixed, particularly with varying quantities of chlorine, sulphate and organic/biological material. The internal mixing state of transported silicate dust (ICE-D) is reported with the sub-composition Chlorine - Org-bio - Nitrate, similar to the treatment of suspended dust in section **??**, except we target nitrate in ambient particles instead of sulphate because nitrate was present in low quantities in suspended soil. An increase in nitrate aerosol has previously been observed in association with air masses passing through Europe and Africa to Cabo Verde (Fomba et al., 2014), so this may be a useful indicator of the history of transported dust.

In transported dust, nitrate mixing with the silicate dust was varied, with the sub-composition of nitrate markers indicating a relatively greater quantity of nitrate mixing with silicate particles during the inter-dust period between the defined dust events. This showed a similar trend to the number concentration of nitrate sea-spray aerosol particle types extracted by fuzzy clustering (Supplement S3.5), which suggest the particles may have co-existed in the same air mass for some period of time. There was a distinct drop in nitrate sub-composition during the dust period D2 when the we also report a change in silicate mineralogy.

Although it is not possible to conclude a primary or secondary processing source of organic/biological mixing, we observed less variation in mixing state in the transported dust than in the laboratory generated reference material. The number of particles whose mixing state sub-composition contained more than $20\%$ organic-biological material (Org-Bio > 0.2) varies with the dust concentration (Fig. 12(d)), and the median amount of organic-biological marker signal is fairly stable, with the exception of a 24 hour period following dust event D1 (Fig. 12(e)). This may be informative of how well mixed local sources of dust become after emission, but could also be a reflection of atmospheric processing.

Particle mixing is important because the efficient ice nucleating properties of proteinaceous INP can be transferred to dust particles after mixing ((Augustin-Bauditz et al., 2016; O'Sullivan et al., 2016)). It is interesting to note that Price et al. (2018) did not see significant variation in INP concentration in aircraft based studies of the Saharan air layer during ICE-D, despite geographically widespread sources of that dust. The origin of the organic-biological markers $CN^-$ and $CNO^-$ in these dust particle requires further investigation. Zawadowicz et al. (2017) demonstrated a method of distinguishing between biogenic and in-organic ion signals using a different SPMS instrument (PALMS), but it is not yet proven to be transferable to other instruments designs.

## 3.4    Potential source areas and transport history

Dust transport to Cabo Verde is controlled by the position of the Azores high pressure system whose anticyclonic flow results in persistent north easterly trade winds along the coast of Morocco, Western Sahara and Mauritania (Carpenter et al., 2010). Dust concentrations at ground level are influenced by the dust deposition rate which is strongly dependent on the horizontal and vertical dust distribution (Schepanski et al., 2009a). We used back trajectory analysis, satellite observations and our measurement of dust mineralogy and mixing state to give potential source areas and transport history of two dust event observed at Cape Verde in the summer of 2015.

Back trajectory analysis of both dust events (D1 and D2, defined in the analysis above), shows transport in the trade winds within the marine boundary (Fig. 13c, g). Influence from the African continent is evident during D1 when some of this air mass was lofted over the Atlas Mountains, Morocco before descending into the marine boundary layer (MBL). The high ISCM ratio we measure $(68\%)$ is consistent with Scheuvens et al. (2013) who suggested illite/kaolinite ratio >2 are indicative of the PSA that comprises the northern part of the west coast of Africa and the south eastern slopes of the Atlas Mountains. Satellite observations at the time showed a plume of dust developing in Algeria and crossing the Atlas mountains and then above the Atlantic Ocean in the days proceeding the dust event D1 (Supplement S5). However, source activation observed by remote satellite is subject to errors associated with the temporal resolution of the measurement (Schepanski et al., 2012). Dust emission associated with density currents related to moist convection has been observed on the Sahara side of the Atlas

Mountain chain (Knippertz et al., 2007), where the soil mineralogy is close match to the material we report in this dust event. The Anti-atlas mountains was also suggested as a source of micronutrients in sediment traps in the North East Atlantic Ocean by Chavagnac et al. (2007).

In contrast, back trajectories for D2 suggest this air mass was never lofted over Africa, but came into direct contact with the coastline of Mauritania. This is a possible source of dust that could explain the relatively low ISCM content and relatively high calcium fraction which is consistent with source sediments of the Atlantic Coastal basin (Moreno et al., 2006). In off-line filters collected at Praia, Cabo Verde, Kandler et al. (2011b) reported illite/kaolinite ratio of between 1:2 and 1:4 during winter transport of dust from coastal Mauritania and Mali respectively.

The nitrate mixing state of particles also suggests different transport pathways for the two dust events. The mixing of nitrate with silicate during and after D1 indicates contact with polluted air, and is consistent with transport from the North, as reported by Salvador et al. (2016), whilst the cleaner particles in D2 indicate that no such mixing took place. An increase in the fraction of sulphate containing sea-spray aerosol in D2 on the other hand (Supplement S3.5) may be associated with organosulfur containing compounds from biogenic sources in the coastal upwelling region off the coast of Mauritania. In addition, the particle size distribution of the silicate from D2 also suggests that this dust may have been transported a relatively short distance compared to D1 (See supplement S4). The silicate from D1 has a well-defined mode at approximately $1\mu m$, which is in contrast to the broader distribution of D2 particle sizes, which extends above $2\mu m$.

Our high resolution measurements show that the mineralogy and mixing sate of dust can change on an hourly basis, suggesting that changes in dust source, transport pathways and particle composition may be lost in off-line data. For example, in XRD analysis of material captured in marine sediment traps of Cape Blanc, Mauritania, Friese et al. (2017) concluded that seasonal variation in mineralogy occurred due to changes in transport pathways; from long-distance transport in the SAL during summertime, to local transport in the trade winds in winter. Our measurements also suggest two pathways for dust arriving at Cabo Verde, but with a much finer temporal resolution. We propose that in August 2015, illite rich dust from the NW margin of the Sahara was advected into the free troposphere and became mixed in to the MBL off the coast of Morocco before several days transport to Cabo Verde. An eastward shift in the Azores high results in the direct entrainment of dust into the MBL from the coast of Mauritania, producing a relatively illite poor and calcium rich dust event in Cabo Verde on 17th August that lasted for a few hours. In all the above off-line studies, filters were exposed for around 1 day resulting in insufficient temporal resolution of the data.

# 4 Conclusions

We present a detailed characterization of the mineralogy and mixing state of the fine fraction ($< 2.5\mu m$) of North African mineral dust using a novel combination of sub-composition and crystal structure analysis with a single particle mass spectrometer. Despite the fact that the technique provides incomplete coverage in terms of particle number, elemental composition, and mineralogy; it was possible to clearly detect regional differences in the mineralogy in single particles of suspended soil and ambient transported dust.

These conclusions were made under the reasonable assumption that single particles in the fine fraction were composed of either clay minerals or feldspars/amorphous matrix, a distinction that can be realised by our novel crystal analysis technique. Although the SPMS technique is shown to be generally non-quantitative with respect to the elemental sub-composition of pure mineral phases such as illite and K-feldspar, a semi-quantitative (relative) measurement of elemental composition can be achieved after particles are separated into mineral groups based on crystal structure. Further differentiation of mineral phase can then be made by comparison to pure mineral fingerprints from within the mineral group. This indicates the importance of particle structure in addition to particle composition in the matrix effect in SPMS.

The sensitivity of the technique to potassium, sodium and aluminum makes it particularly useful for differentiating illite (potassium-rich clay), montmorillonite (sodium-rich clay) and kaolinite (aluminum-rich clay) clay mineral assemblages. Comparison with off-line SEM EDX analysis of the suspended soil confirms the observations of a composition close to illite is observed in Moroccan samples compared to a kaolinite composition in samples from the Sahel, in agreement with geology of these regions. SPMS is less effective than SEM EDX at identifying particles rich in magnesium and calcium due to suppression by the matrix effect and interference from poorly resolved peaks, but it is likely that these elements are derived from carbonates and oxides and are not strictly necessary to classify the silicate minerals. This makes the assumption that Mg, Fe and Ca are of minor importance in silicate mineralogy in continental sediment, which is certainly not true on a local level. However, our measurement show it is not necessary to include this when considering the genesis and subsequent weathering history of the clay fraction in soil on a continental scale.

These results show that the SPMS and SEM EDX techniques are complimentary, with SPMS providing a high resolution on-line indication of mineralogy and mixing state of the principal particle matrix, and SEM EDX providing semi-quantitative elemental composition of all particles, including material that the SPMS may not ablate. In most cases, both techniques show the distribution of mineralogical composition is more continuous than clustered in distinct mineral phases, and only laboratory suspended river sediment from the Anti-Atlas Mountains, Morocco contained a distinct mode of fine particles with a feldspar matrix.

The detailed analysis of laboratory suspended dust provided useful reference data for the interpretation of the origins and transport history of ambient dust in the remote North Atlantic. Although semi-quantitative in terms of particle number fractions due to number counting bias effects associated with instrument function, the relative temporal trends are very informative. A relatively large numbers of illite rich particles (ISCM Ratio > 5) suggests a dust source on the NW margins of the Sahara during the summer. However, a rapid change (< 1 hour) towards a felsic/amorphous particle matrix (ISCM Ratio < 1) was observed in silicate particles when back-trajectories suggest direct emission into the marine boundary layer from the West African coast. This episode lasted only a few hours and challenges previous findings from off-line measurements that the source and composition of transported dust only change on a seasonal basis.

Internal mixing state was of some use to understanding transport history of ambient dust, but must be used with caution because some degree of mixing was already present in the primary soil. However, variations in internally mixed nitrate suggested dust from the NW margins of the Sahara was deposited into the marine boundary layer after transport in the Saharan air layer. In contrast, the relative concentration of organic/biological markers did not vary significantly in transported dust,

but had significant local variation in suspended soil samples, making them less useful for interpreting transport pathways, but potentially informative of how well mixed local sources become after emission. The primary and secondary origin of these chemical markers and how they change the physiochemical properties of dust particles requires further investigation.

The combination of on-line mineralogy and mixing state of ambient dust has potential for resolving the complexity of dust emission, transport and deposition, but more high resolution measurements at varying distance from potential dust sources are required to fully understand the complexity of these processes. The example of transported dust provided here should also be useful for studies of ice nucleation, radiative effects, and heterogeneous reactions involving mineral dust.

*Data availability.* LAAPTOF soil dust characterisation data collected for the INUIT09 campaign at the AIDA facility is available at https://data.eurochamp.org/data-access. Data collected during the ICE-D campaign are available from the British Atmospheric Data Centre, Centre for Environmental Data Analysis (2018, http://www.ceda.ac.uk/), at the following URL: http://catalogue.ceda.ac.uk/uuid/d7e02c75191a4515a28a2( (Bennett, 2018).

*Author contributions.* The document was principally written by N.Marsden with input from R.Ullrich and S.Eriksen Hammer. The INUIT09 project was devised and managed by R.Ullrich and O. Möhler, with SPMS data acquired by N.Marsden. The ICE-D field data was acquired by N.Marsden and P.Williams with support from M. Flynn, J.Allan and H.Coe. Data processing was performed by N.Marsden (SPMS) and S.Eriksen Hammer (ESEM) with support from K.Kandler. Back trajectory analysis by D.Liu and Z.Cui

*Competing interests.* No competing interests declared.

*Disclaimer.* TEXT

*Acknowledgements.* ICE-D was supported by the Natural Environment Research Council (grant number NE/M001954/1), during which N.Marsden was supported by a PhD studentship (NERC M113463J). This project/work has received funding from the European Union's Horizon 2020 research and innovation programme through the EUROCHAMP-2020 Infrastructure Activity under grant agreement No 730997. We thank the AIDA engineering and technical team for maintaining and operating the cloud chamber facility. R. Ullrich and O. Möhler acknowledge funding by the Deutsche Forschungsgemeinschaft (DFG) through the research unit INUIT (FOR 1525, project MO 668/4-2)K. Kandler and S. E. Hammer acknowledge financial support from the Deutsche Forschungsgemeinschaft (DFG, German Research Foundation) – 264907654; 264912134; 416816480 (KA 2280) as well as FOR 1525).

(a)
1:1 Layer Clay

(b)
2:1 Layer Clay

(c)
Framework
Silicate

kaolinite
$Al_2Si_2O_5(OH)_4$

illite
$K_{1.5-1.0}Al_4[Si_{6.5-7.0}Al_{1.5-1.0}O_{20}](OH)_4$

K-feldspar
$K[AlSi_3O_8]$
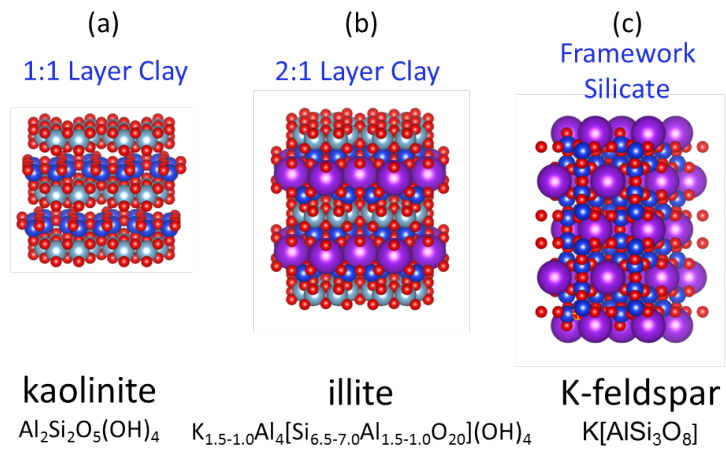
**Figure 1.** The crystal structures of common aluminosilicate minerals (a) 1:1 clay mineral structure of kaolinite, (b) the 2:1 clay mineral structure of illite and (c) the framework structure of k-feldspar. Color code is as follows; Red = anions (O, OH), Grey = octohedral co-ordination (Al, Mg), Blue = tetrahedral co-ordination (Si, Al), purple = interstitial complex (K, Na, Ca).
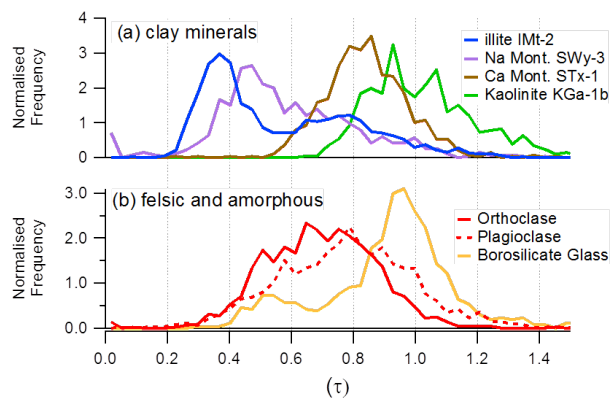
**Figure 2.** The differentiation of reference minerals using crystal structure analysis described by Marsden et al. (2018). The peak shift ratios ($\tau$) were calculated from ion arrival times from individual particles in the mass spectrometer, rather than conventional peak area analysis for elemental composition. Nominally pure mineral dust was sampled after dispersed in a dust tower (a) nominally pure clay minerals from the clay mineral society and (b) orthoclase (K feldspar), plagioclase (Na feldspar) and borosilicate glass.
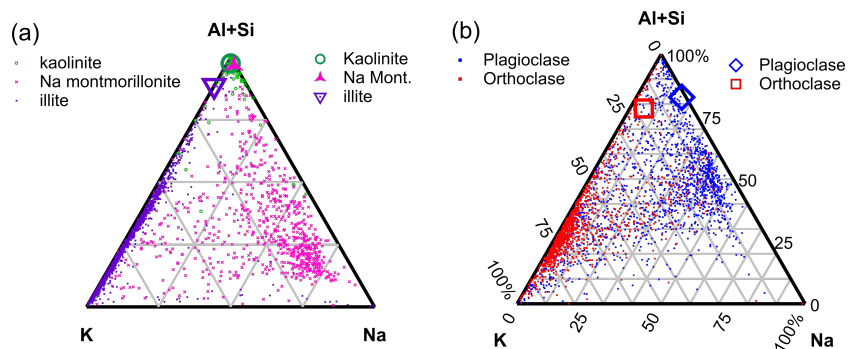
**Figure 3.** The differentiation of reference minerals using sub-compositional analysis. Each dot in the ternary plots represents the composition of a single particle calculated from Al+Si, K and Na peak areas in the mass spectra. Larger icons represent bulk composition by XRF analysis. Nominally pure mineral dust was sampled after dispersed in a dust tower (a) nominally pure clay minerals illite (1806), kaolinite (1388 particles) and Na-montmorillonite (800 particles) from the clay mineral society and (b) orthoclase (K feldspar, 1318 particles) and plagioclase (Na feldspar, 1568 particles).
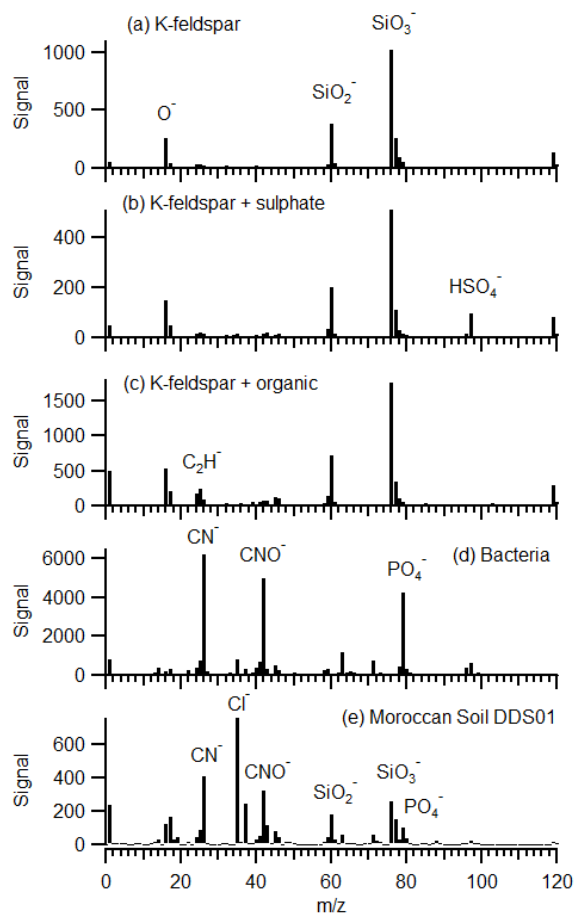
**Figure 4.** Average negative ion mass spectra (200 particles) of re-suspended material in the AIDA chamber during the FIN-1 campaign. (a) pure K-feldspar, (b) K-feldspar with sulfate coating, (c) K-feldspar with organic coating, (d) bacteria and (d) Moroccan soil dust DDS01 during INUIT09.
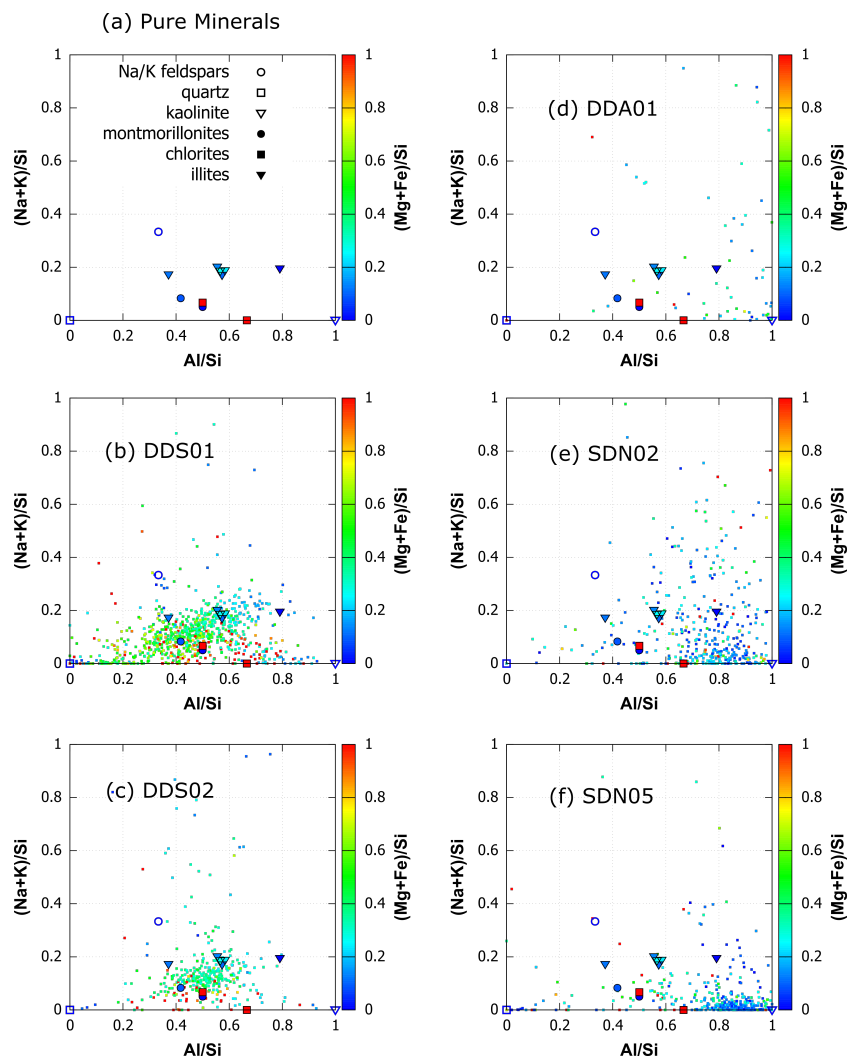
**Figure 5.** Elemental sub-composition diagrams of suspended natural soil samples (INUIT09) by SEM EDX analysis. (a) average composition of nominally pure mineral samples, (b) DDS01, (c) DDS02, (d) DDA01, (e) SDN02, (f) SDN05. Ratios are calculated from atomic %
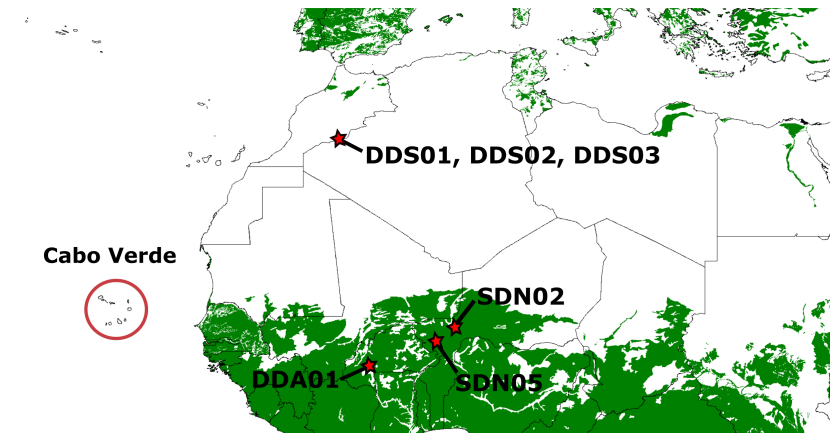
**Figure 6.** Sampling locations of natural soil (stars) and transported dust at Cabo Verde (circle). The green color indicates soils that have a cation ion exchange capacity (CEC) of less than 35 cmol/kg indicating kaolinite rich soil. Produced from the Digital Soil Map of the World.
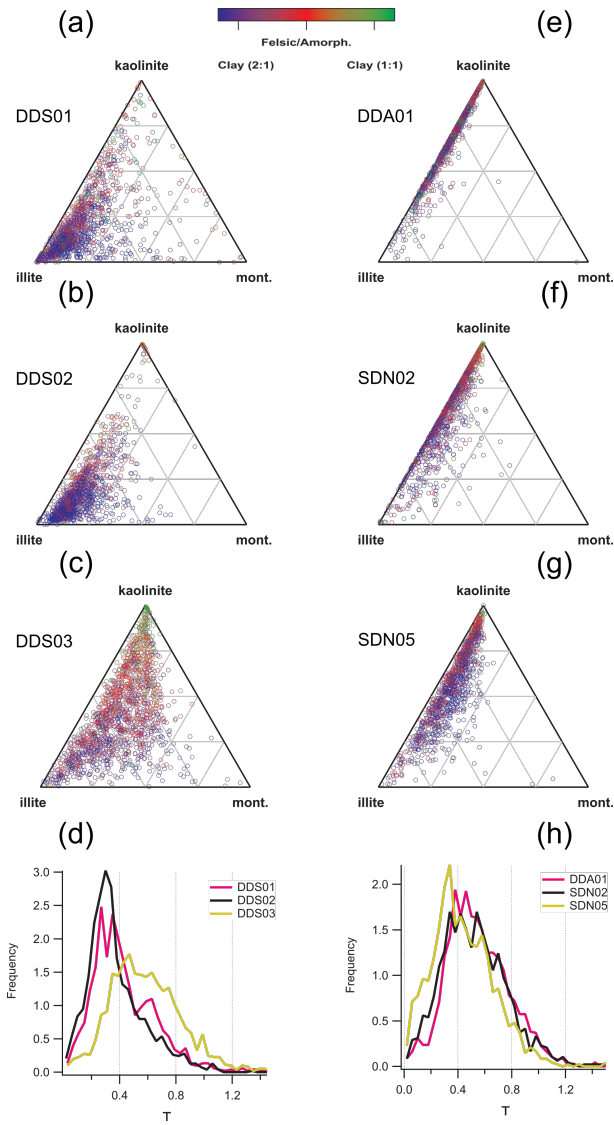
**Figure 7.** Sub-compositional analysis of suspended natural soil samples (INUIT09) by SPMS. The ternary diagrams are referenced to the inferred kaolinite, illite, Na-montmorillonite end members of the clay mineral series using the Al+Si, K, and Na ratios from reference minerals (Fig. 3) . Samples from Morocco in the left column (a, b, c), and samples from the Sahel in the right column (e, f, g). The color function is proportional to the $\tau$ parameter as defined by the crystal structure analysis technique, so that the blue dots represent 2:1 clay minerals The distribution of $\tau$ for each sample is also displayed as a histogram (d, h). (2000 particles analysed in each sample)
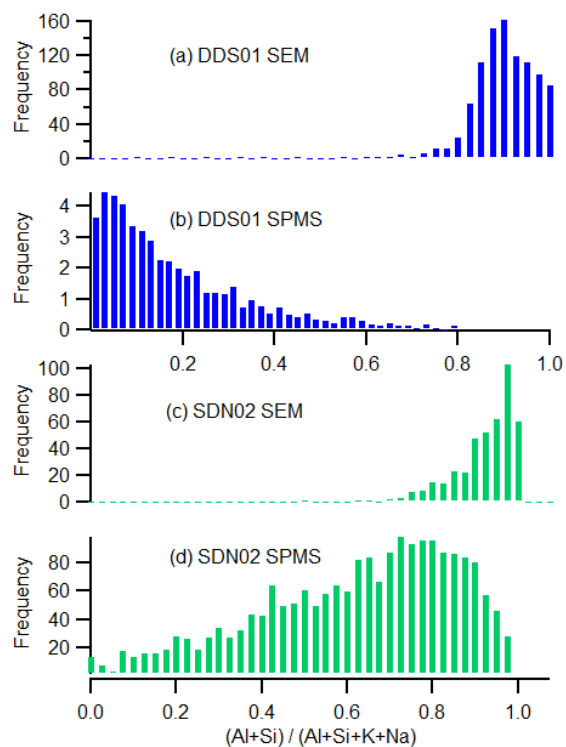
**Figure 8.** A comparison of the relative sensitivity of the SPMS and SEM techniques to the principal elements in silicate minerals. Histograms represent the sensitivity to alkali metals of the interstitial complex with respect to the Al and Si of the silicate structure ((Al+Si)/(Al+Si+K+Na)) in single particles. Moroccan soil sample DDS01 (a, b) compared to Sahelian soil sample SDN02 (c, d) using the SEM and SPMS technique respectively.
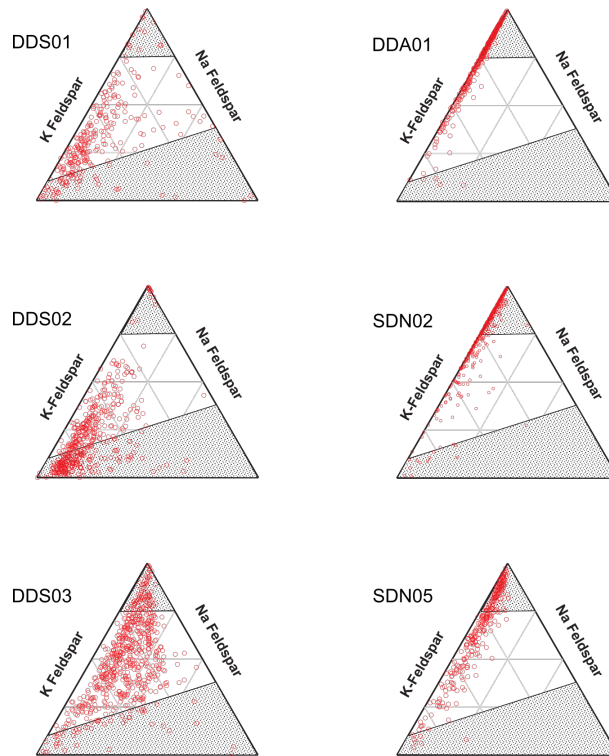
**Figure 9.** Sub-compositional analysis of the feldspar/amorphous content in suspended natural soil samples (INUIT09) by SPMS. The felsic/amorphous fraction was selected by crystal structure analysis ($\tau = 0.58 - 0.8$). The ternary diagrams are referenced to the inferred K and Na end members of the feldspar series using the Al+Si, K, and Na ratios from reference minerals (Fig. 3). The greyed out area represent unlikely composition of feldspar as demonstrated by the reference minerals. Samples from Morocco in the left column (a, b, c), and samples from the Sahel in the right column (e, f, g)
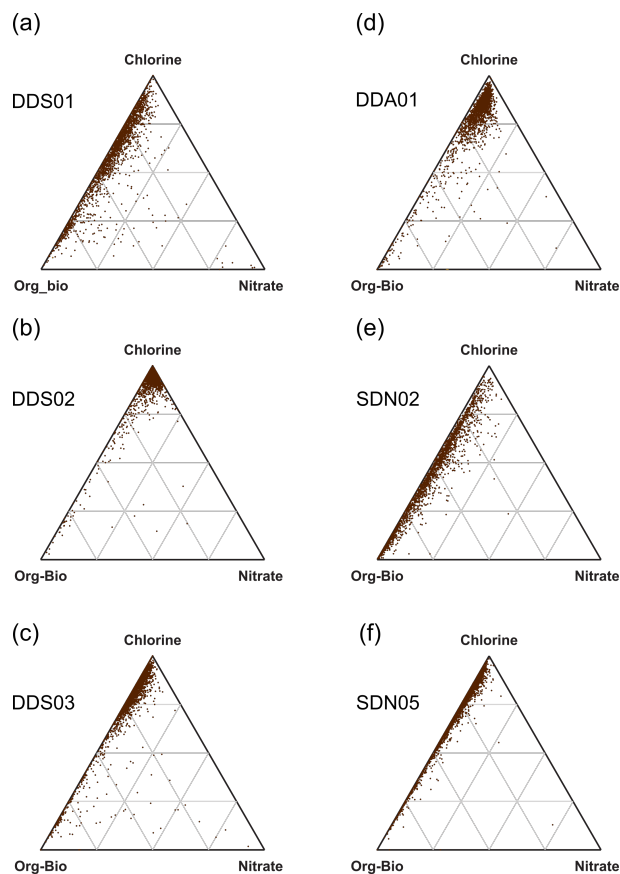
**Figure 10.** Sub-compositional analysis of the non-silicate content in suspended natural soil samples (INUIT09) by SPMS. Ternary plots of the Cl, organic-biological and sulphate marker peak areas in Moroccan (a, b, c) and Sahelian (c, d, e) re-suspended soil dust. (2000 particles analysed in each sample)
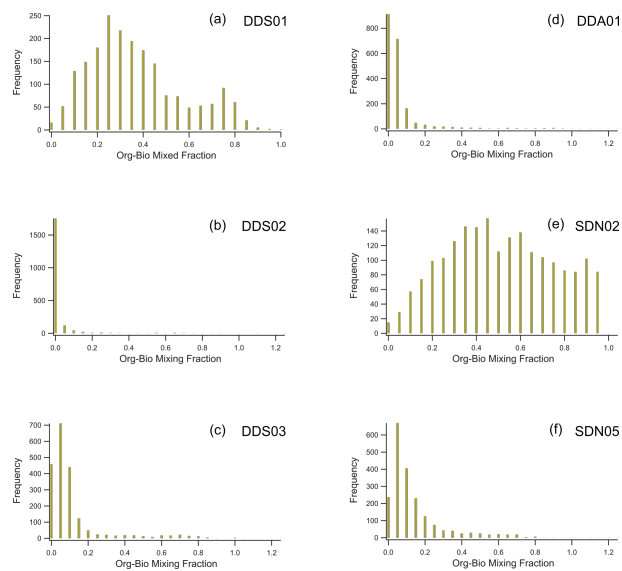
**Figure 11.** A comparison of the relative organic/biological content in the non-silicate portion in suspended natural soil samples (INUIT09). Histograms are of the normalised Org-Bio fraction in single particles of Moroccan (a, b, c) and Sahelian (d, e, f) samples.
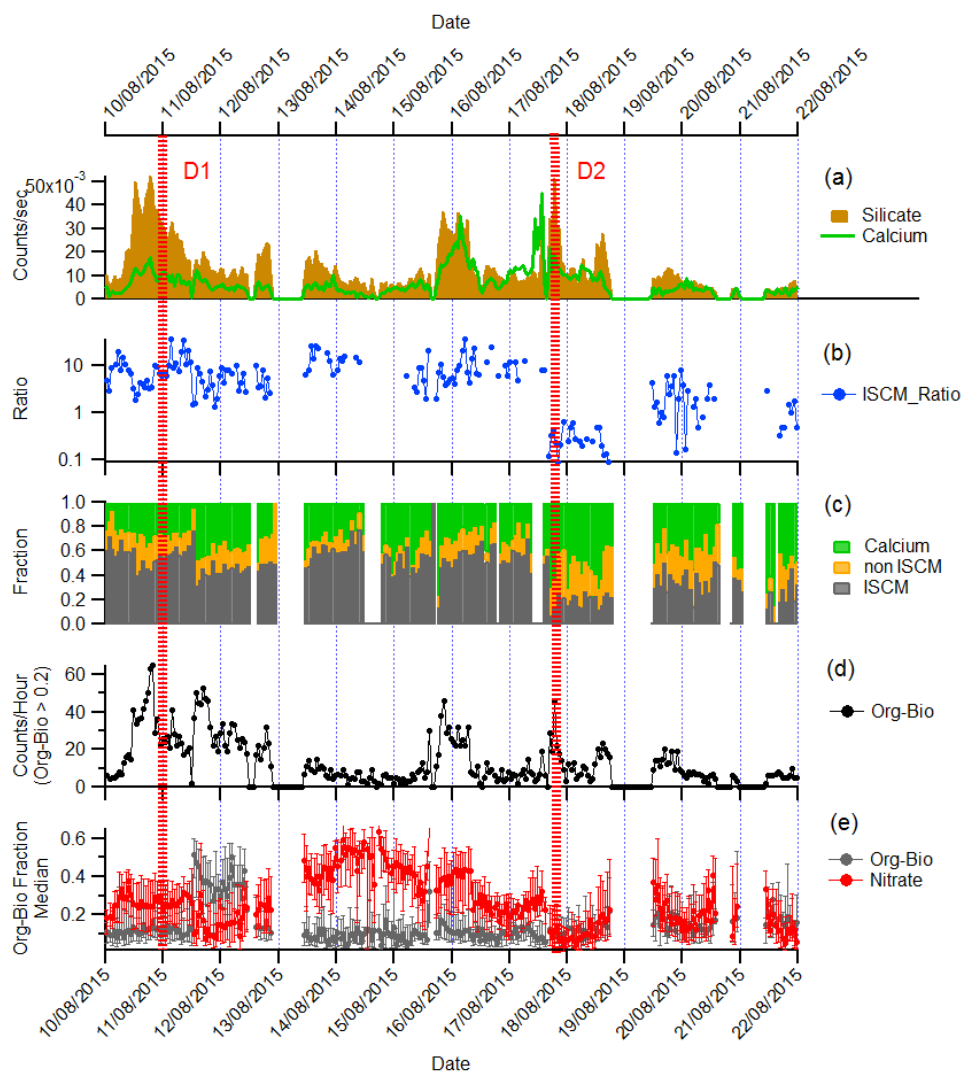
**Figure 12.** Time series (1 hour resolution) of ambient dust properties measured at Cabo Verde during the ICE-D campaign by LAAPTOF SPMS. A total of 12698 (a) concentration of silicate and calcium rich particles (total measurement of 12698 silicate and 6837 calcium rich particles). (b) Hourly average ratio of ISCM to non-ISCM minerals (ISCM Ratio) determined by crystal structure, (c) Hourly particle number fraction of calcium, ISCM and non-ISCM particles. (d) Hourly concentration of silicate particles with organic-biological sub-composition > 0.2. (e) Hourly median Org-Bio and nitrate sub-composition marker quantity. Error bar is 25th and 75th percentile.
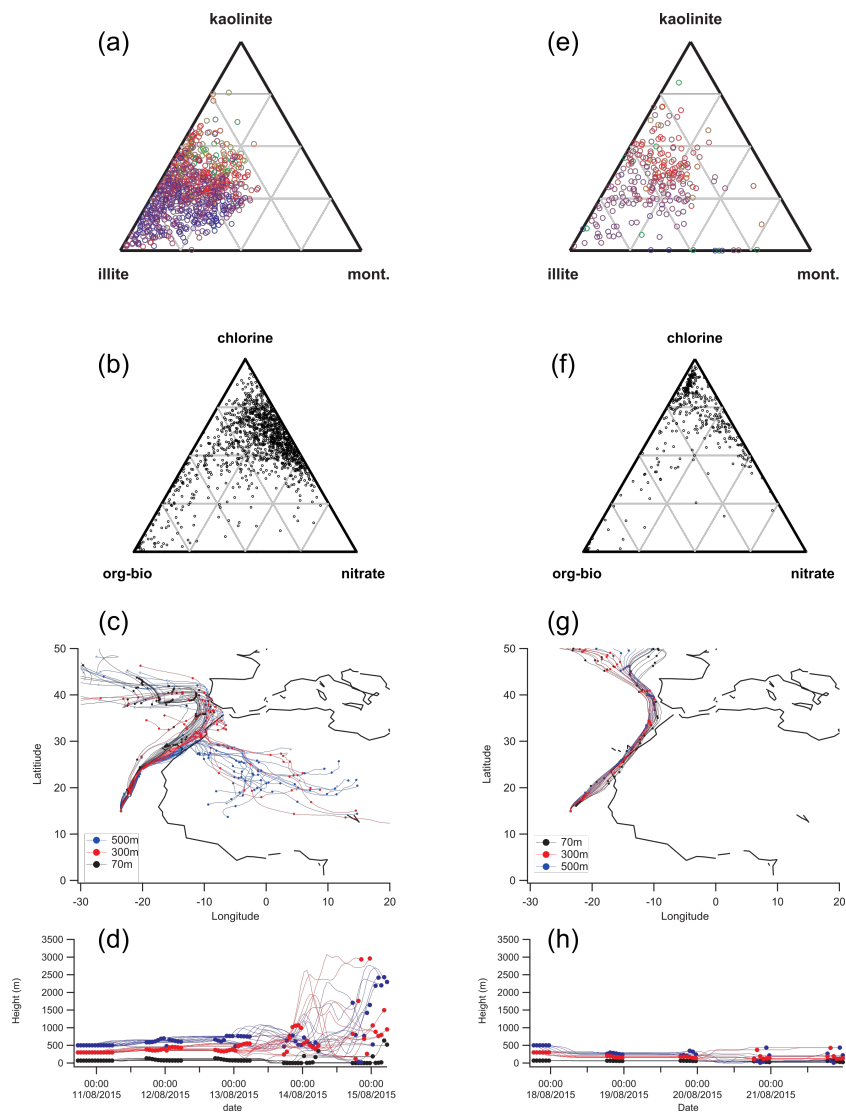
**Figure 13.** Analysis of the mineralogy and mixing state of dust events D1 in the left column (a-d) (1301 dust particle analysed) and D2 in the right column (e-f)(378 particles analysed). Mineralogical analysis by SPMS shows the high number of illite particles (blue circles) present in D1 (a) are absent in D2 (e). In addition, mixing state analsyis shows a higher proportion of particles mixed with nitrate in D1 (d) than in D2 (f). HYSPLIT back trajectory analysis suggest influence of air masses from the Sahara during D1 (c,d) and coastal Mauritania during D2 (g,h).

# References

Ahern, A., Subramanian, R., Saliba, G., Lipsky, E. M., Donahue, N. M., and Sullivan, R. C.: Effect of secondary organic aerosol coating thickness on the real-time detection and characterization of biomass-burning soot by two particle mass spectrometers, Atmospheric Measurement Techniques, 9, 6117–6137, https://doi.org/10.5194/amt-9-6117-2016, http://www.atmos-meas-tech-discuss.net/amt-2016-201/, 2016.

Ansmann, A., Petzold, A., Kandler, K., Tegen, I., Wendisch, M., Müller, D., Weinzierl, B., Müller, T., and Heintzenberg, J.: Saharan Mineral Dust Experiments SAMUM-1 and SAMUM-2: what have we learned?, Tellus B, 63, 403–429, https://doi.org/10.1111/j.1600-0889.2011.00555.x, http://www.tellusb.net/index.php/tellusb/article/view/16236, 2011.

Atkinson, J. D., Murray, B. J., Woodhouse, M. T., Whale, T. F., Baustian, K. J., Carslaw, K. S., Dobbie, S., O'Sullivan, D., and Malkin, T. L.: The importance of feldspar for ice nucleation by mineral dust in mixed-phase clouds., Nature, 498, 355–358, https://doi.org/10.1038/nature12278, http://www.ncbi.nlm.nih.gov/pubmed/23760484, 2013.

Augustin-Bauditz, S., Wex, H., Denjean, C., Hartmann, S., Schneider, J., Schmidt, S., Ebert, M., and Stratmann, F.: Laboratory-generated mixtures of mineral dust particles with biological substances: Characterization of the particle mixing state and immersion freezing behavior, Atmospheric Chemistry and Physics, 16, 5531–5543, https://doi.org/10.5194/acp-16-5531-2016, 2016.

Baker, A. R., Kelly, S., Biswas, K., Witt, M., and Jickells, T.: Atmospheric deposition of nutrients to the Atlantic Ocean, Geophysical Research Letters, 30, 2–5, https://doi.org/10.1029/2003GL018518, 2003.

Baustian, K. J., Cziczo, D. J., Wise, M. E., Pratt, K. a., Kulkarni, G., Hallar, a. G., and Tolbert, M. a.: Importance of aerosol composition, mixing state, and morphology for heterogeneous ice nucleation: A combined field and laboratory approach, Journal of Geophysical Research, 117, D06 217, https://doi.org/10.1029/2011JD016784, http://doi.wiley.com/10.1029/2011JD016784, 2012.

Bhave, P. V., Allen, J. O., Morrical, B. D., Fergenson, D. P., Cass, G. R., and Prather, K. a.: A field-based approach for deterimining ATOFMS instrument sensitivities to ammonium and nitrate., Environmental science & technology, 36, 4868–4879, 2002.

Cahill, J. F., Suski, K., Seinfeld, J. H., Zaveri, R. a., and Prather, K. a.: The mixing state of carbonaceous aerosol particles in northern and southern California measured during CARES and CalNex 2010, Atmospheric Chemistry and Physics, 12, 10 989–11 002, https://doi.org/10.5194/acp-12-10989-2012, http://www.atmos-chem-phys.net/12/10989/2012/, 2012.

Caponi, L., Formenti, P., Massabó, D., Di Biagio, C., Cazaunau, M., Pangui, E., Chevaillier, S., Landrot, G., Andreae, O. M., Kandler, K., Piketh, S., Saeed, T., Seibert, D., Williams, E., Balkanski, Y., Prati, P., and Doussin, J. F.: Spectral- and size-resolved mass absorption efficiency of mineral dust aerosols in the shortwave spectrum: A simulation chamber study, Atmospheric Chemistry and Physics, 17, 7175–7191, https://doi.org/10.5194/acp-17-7175-2017, 2017.

Caquineau, S., Gaudichet, A., Gomes, L., and Legrand, M.: Mineralogy of Saharan dust transported over northwestern tropical Atlantic Ocean in relation to source regions, Journal of Geophysical Research Atmospheres, 107, https://doi.org/10.1029/2000JD000247, 2002.

Carpenter, L. J., Fleming, Z. L., Read, K. A., Lee, J. D., Moller, S. J., Hopkins, J. R., Purvis, R. M., Lewis, A. C., Müller, K., Heinold, B., Herrmann, H., Fomba, K. W., Van Pinxteren, D., Müller, C., Tegen, I., Wiedensohler, A., Müller, T., Niedermeier, N., Achterberg, E. P., Patey, M. D., Kozlova, E. A., Heimann, M., Heard, D. E., Plane, J. M. C., Mahajan, A., Oetjen, H., Ingham, T., Stone, D., Whalley, L. K., Evans, M. J., Pilling, M. J., Leigh, R. J., Monks, P. S., Karunaharan, A., Vaughan, S., Arnold, S. R., Tschritter, J., Pöhler, D., Frieã, U., Holla, R., Mendes, L. M., Lopez, H., Faria, B., Manning, A. J., and Wallace, D. W. R.: Seasonal characteristics of tropical marine boundary layer air measured at the cape verde atmospheric observatory, Journal of Atmospheric Chemistry, 67, 87–140, https://doi.org/10.1007/s10874-011-9206-1, 2010.

Carslaw, K. S., Lee, L. a., Reddington, C. L., Pringle, K. J., Rap, a., Forster, P. M., Mann, G. W., Spracklen, D. V., Woodhouse, M. T., Regayre, L. a., and Pierce, J. R.: Large contribution of natural aerosols to uncertainty in indirect forcing., Nature, 503, 67–71, https://doi.org/10.1038/nature12674, http://www.ncbi.nlm.nih.gov/pubmed/24201280, 2013.

Chavagnac, V., Waniek, J. J., Atkin, D., Milton, J. A., Leipe, T., Green, D. R., Bahlo, R., Hayes, T. E., and Schulz-Bull, D. E.: Anti-Atlas Moroccan Chain as the source of lithogenic-derived micronutrient fluxes to the deep Northeast Atlantic Ocean, Geophysical Research Letters, 34, 1–5, https://doi.org/10.1029/2007GL030985, 2007.

Christopoulos, C. D., Garimella, S., Zawadowicz, M. A., Möhler, O., and Cziczo, D. J.: A machine learning approach to aerosol classification for single-particle mass spectrometry, Atmospheric Measurement Techniques, 11, 5687–5699, https://doi.org/10.5194/amt-11-5687-2018, https://www.atmos-meas-tech-discuss.net/amt-2017-468/amt-2017-468.pdf, 2018.

Claquin, T., Schulz, M., and Balkanski, Y. J.: Modeling the mineralogy of atmospheric dust sources, Journal of Geophysical Research, 104, 22 243, https://doi.org/10.1029/1999JD900416, http://doi.wiley.com/10.1029/1999JD900416, 1999.

Connolly, P. J., Möhler, O., Field, P. R., Saathoff, H., Burgess, R., Choularton, T., and Gallagher, M.: Studies of heterogeneous freezing by three different desert dust samples, Atmospheric Chemistry and Physics, 9, 2805–2824, https://doi.org/10.5194/acp-9-2805-2009, http://www.atmos-chem-phys-discuss.net/9/463/2009/, 2009.

Creamean, J. M., Suski, K. J., Rosenfeld, D., Cazorla, A., Demott, P. J., Sullivan, R. C., White, A. B., Ralph, F., Minnis, P., Comstock, J. M., Tomlinson, J. M., and Prather, K. A.: Dust and Biological Aerosols, Science (New York, N.Y.), 339, 1572–1578, https://doi.org/10.1126/science.1227279, 2013.

Cziczo, D. J., DeMott, P. J., Brock, C., Hudson, P. K., Jesse, B., Kreidenweis, S. M., Prenni, a. J., Schreiner, J., Thomson, D. S., and Murphy, D. M.: A Method for Single Particle Mass Spectrometry of Ice Nuclei, Aerosol Science and Technology, 37, 460–470, https://doi.org/10.1080/02786820300976, 2003.

Cziczo, D. J., Thomson, D. S., Thompson, T. L., DeMott, P. J., and Murphy, D. M.: Particle analysis by laser mass spectrometry (PALMS) studies of ice nuclei and other low number density particles, International Journal of Mass Spectrometry, 258, 21–29, https://doi.org/10.1016/j.ijms.2006.05.013, http://linkinghub.elsevier.com/retrieve/pii/S1387380606002636, 2006.

Cziczo, D. J., Froyd, K. D., Gallavardin, S. J., Moehler, O., Benz, S., Saathoff, H., and Murphy, D. M.: Deactivation of ice nuclei due to atmospherically relevant surface coatings, Environmental Research Letters, 4, 044 013, https://doi.org/10.1088/1748-9326/4/4/044013, http://stacks.iop.org/1748-9326/4/i=4/a=044013?key=crossref.f0b33c2dbaef8b0dc49fb4ee48d5bf82, 2009.

Dall'Osto, M., Harrison, R. M., Highwood, E. J., O'Dowd, C., Ceburnis, D., Querol, X., and Achterberg, E. P.: Variation of the mixing state of Saharan dust particles with atmospheric transport, Atmospheric Environment, 44, 3135–3146, https://doi.org/10.1016/j.atmosenv.2010.05.030, http://dx.doi.org/10.1016/j.atmosenv.2010.05.030, 2010.

DeMott, P. J.: African dust aerosols as atmospheric ice nuclei, Geophysical Research Letters, 30, 1732, https://doi.org/10.1029/2003GL017410, http://doi.wiley.com/10.1029/2003GL017410, 2003.

DeMott, P. J., Prenni, a. J., Liu, X., Kreidenweis, S. M., Petters, M. D., Twohy, C. H., Richardson, M. S., Eidhammer, T., and Rogers, D. C.: Predicting global atmospheric ice nuclei distributions and their impacts on climate., Proceedings of the National Academy of Sciences of the United States of America, 107, 11 217–22, https://doi.org/10.1073/pnas.0910818107, http://www.pubmedcentral.nih.gov/articlerender.fcgi?artid=2895116&tool=pmcentrez&rendertype=abstract, 2010.

Di Biagio, C., Formenti, P., Balkanski, Y., Caponi, L., Cazaunau, M., Pangui, E., Journet, E., Nowak, S., Caquineau, S., Andreae O, M., Kandler, K., Saeed, T., Piketh, S., Seibert, D., Williams, E., and Doussin, J. F. C.: Global scale variability of the mineral dust long-wave

refractive index: A new dataset of in situ measurements for climate modeling and remote sensing, Atmospheric Chemistry and Physics, 17, 1901–1929, https://doi.org/10.5194/acp-17-1901-2017, 2017.

Doherty, O. M., Riemer, N., and Hameed, S.: Saharan mineral dust transport into the Caribbean: Observed atmospheric controls and trends, Journal of Geophysical Research Atmospheres, 113, 1–10, https://doi.org/10.1029/2007JD009171, 2008.

5    Dunion, J. P. and Marron, C. S.: A reexamination of the Jordan mean tropical sounding based on awareness of the Saharan air layer: Results from 2002, Journal of Climate, 21, 5242–5253, https://doi.org/10.1175/2008JCLI1868.1, 2008.

Engelbrecht, J. P., Moosmüller, H., Pincock, S., Jayanty, R. K., Lersch, T., and Casuccio, G.: Technical note: Mineralogical, chemical, morphological, and optical interrelationships of mineral dust re-suspensions, Atmospheric Chemistry and Physics, 16, 10 809–10 830, https://doi.org/10.5194/acp-16-10809-2016, http://www.atmos-chem-phys-discuss.net/acp-2016-286/, 2016.

10    Evan, A. T., Flamant, C., Fiedler, S., and Doherty, O.: An analysis of aeolian dust in climate models, Geophysical Research Letters, 41, 5996–6001, https://doi.org/10.1002/2014GL060545, 2014.

Fitzgerald, E., Ault, A. P., Zauscher, M. D., Mayol-Bracero, O. L., and Prather, K. a.: Comparison of the mixing state of long-range transported Asian and African mineral dust, Atmospheric Environment, 115, 19–25, https://doi.org/10.1016/j.atmosenv.2015.04.031, http://linkinghub.elsevier.com/retrieve/pii/S1352231015300340, 2015.

15    Fomba, K. W., Müller, K., Van Pinxteren, D., Poulain, L., Van Pinxteren, M., and Herrmann, H.: Long-term chemical characterization of tropical and marine aerosols at the Cape Verde Atmospheric Observatory (CVAO) from 2007 to 2011, Atmospheric Chemistry and Physics, 14, 8883–8904, https://doi.org/10.5194/acp-14-8883-2014, 2014.

Formenti, P., Schütz, L., Balkanski, Y., Desboeufs, K., Ebert, M., Kandler, K., Petzold, A., Scheuvens, D., Weinbruch, S., and Zhang, D.: Recent progress in understanding physical and chemical properties of African and Asian mineral dust, Atmospheric Chemistry and

20    Physics, 11, 8231–8256, https://doi.org/10.5194/acp-11-8231-2011, 2011.

Formenti, P., Caquineau, S., Desboeufs, K., Klaver, A., Chevaillier, S., Journet, E., and Rajot, J. L.: Mapping the physico-chemical properties of mineral dust in western Africa: Mineralogical composition, Atmospheric Chemistry and Physics, 14, 10 663–10 686, https://doi.org/10.5194/acp-14-10663-2014, 2014.

Friese, C. A., Van Hateren, J. A., Vogt, C., Fischer, G., and Stuut, J. B. W.: Seasonal provenance changes in present-day Saharan dust collected

25    in and off Mauritania, Atmospheric Chemistry and Physics, 17, 10 163–10 193, https://doi.org/10.5194/acp-17-10163-2017, 2017.

Gallavardin, S. J., Froyd, K. D., Lohmann, U., Moehler, O., Murphy, D. M., and Cziczo, D. J.: Single Particle Laser Mass Spectrometry Applied to Differential Ice Nucleation Experiments at the AIDA Chamber, Aerosol Science and Technology, 42, 773–791, https://doi.org/10.1080/02786820802339538, http://www.tandfonline.com/doi/abs/10.1080/02786820802339538, 2008.

Gaston, C. J., Quinn, P. K., Bates, T. S., Gilman, J. B., Bon, D. M., Kuster, W. C., and Prather, K. a.: The impact of shipping, agricultural,

30    and urban emissions on single particle chemistry observed aboard the R/V Atlantis during CalNex, Journal of Geophysical Research: Atmospheres, 118, 5003–5017, https://doi.org/10.1002/jgrd.50427, http://doi.wiley.com/10.1002/jgrd.50427, 2013.

Gemayel, R., Hellebust, S., Temime-Roussel, B., Hayeck, N., Van Elteren, J. T., Wortham, H., and Gligorovski, S.: The performance and the characterization of laser ablation aerosol particle time-of-flight mass spectrometry (LAAP-ToF-MS), Atmospheric Measurement Techniques, 9, 1947–1959, https://doi.org/10.5194/amt-9-1947-2016, 2016.

35    Glaccum, R. A. and Prospero, J. M.: Saharan aerosols over the tropical North Atlantic — Mineralogy, Marine Geology, 37, 295–321, https://doi.org/10.1016/0025-3227(80)90107-3, http://www.sciencedirect.com/science/article/pii/0025322780901073, 1980.

Griffin, D. W.: Atmospheric movement of microorganisms in clouds of desert dust and implications for human health., Clinical microbiology reviews, 20, 459–77, https://doi.org/10.1128/CMR.00039-06, http://www.pubmedcentral.nih.gov/articlerender.fcgi?artid=1932751&tool=pmcentrez&rendertype=abstract, 2007.

Gross, D. S., Gälli, M. E., Silva, P. J., and Prather, K. a.: Relative sensitivity factors for alkali metal and ammonium cations in single-particle aerosol time-of-flight mass spectra., Analytical chemistry, 72, 416–22, http://www.ncbi.nlm.nih.gov/pubmed/10658339, 2000.

Gross, D. S., Atlas, R., Rzeszotarski, J., Turetsky, E., Christensen, J., Benzaid, S., Olson, J., Smith, T., Steinberg, L., and Sulman, J.: Environmental chemistry through intelligent atmospheric data analysis, Environmental Modelling & Software, 25, 760–769, https://doi.org/10.1016/j.envsoft.2009.12.001, http://linkinghub.elsevier.com/retrieve/pii/S1364815209003041, 2010.

Hammer, S. E., Mertes, S., Schneider, J., Ebert, M., Kandler, K., and Weinbruch, S.: Composition of ice particle residuals in mixed-phase clouds at Jungfraujoch (Switzerland): Enrichment and depletion of particle groups relative to total aerosol, Atmospheric Chemistry and Physics, 18, 13 987–14 003, https://doi.org/10.5194/acp-18-13987-2018, 2018.

Harrison, A. D., Whale, T. F., Carpenter, M. A., Holden, M. A., Neve, L., O'Sullivan, D., Vergara Temprado, J., and Murray, B. J.: Not all feldspars are equal: A survey of ice nucleating properties across the feldspar group of minerals, Atmospheric Chemistry and Physics, 16, 10 927–10 940, https://doi.org/10.5194/acp-16-10927-2016, 2016.

Hatch, L. E., Pratt, K. a., Huffman, J. A., Jimenez, J. L., and Prather, K. a.: Impacts of Aerosol Aging on Laser Desorption/Ionization in Single-Particle Mass Spectrometers, Aerosol Science and Technology, 48, 1050–1058, https://doi.org/10.1080/02786826.2014.955907, http://www.tandfonline.com/doi/abs/10.1080/02786826.2014.955907, 2014.

Heinold, B., Knippertz, P., Marsham, J. H., Fiedler, S., Dixon, N. S., Schepanski, K., Laurent, B., and Tegen, I.: The role of deep convection and nocturnal low-level jets for dust emission in summertime West Africa: Estimates from convection-permitting simulations, Journal of Geophysical Research Atmospheres, 118, 4385–4400, https://doi.org/10.1002/jgrd.50402, 2013.

Hinz, K.-P., Erdmann, N., Grüning, C., and Spengler, B.: Comparative parallel characterization of particle populations with two mass spectrometric systems LAMPAS 2 and SPASS, International Journal of Mass Spectrometry, 258, 151–166, https://doi.org/10.1016/j.ijms.2006.09.008, http://linkinghub.elsevier.com/retrieve/pii/S1387380606004246, 2006.

Hiranuma, N., Augustin-Bauditz, S., Bingemer, H., Budke, C., Curtius, J., Danielczok, A., Diehl, K., Dreischmeier, K., Ebert, M., Frank, F., Hoffmann, N., Kandler, K., Kiselev, A., Koop, T., Leisner, T., Möhler, O., Nillius, B., Peckhaus, A., Rose, D., Weinbruch, S., Wex, H., Boose, Y., Demott, P. J., Hader, J. D., Hill, T. C., Kanji, Z. A., Kulkarni, G., Levin, E. J., McCluskey, C. S., Murakami, M., Murray, B. J., Niedermeier, D., Petters, M. D., O'Sullivan, D., Saito, A., Schill, G. P., Tajiri, T., Tolbert, M. A., Welti, A., Whale, T. F., Wright, T. P., and Yamashita, K.: A comprehensive laboratory study on the immersion freezing behavior of illite NX particles: A comparison of 17 ice nucleation measurement techniques, Atmospheric Chemistry and Physics, 15, 2489–2518, https://doi.org/10.5194/acp-15-2489-2015, 2015.

Hoose, C. and Mohler, O.: Heterogeneous ice nucleation on atmospheric aerosols: a review of results from laboratory experiments, Atmospheric Chemistry and Physics, 12, 9817–9854, https://doi.org/10.5194/acp-12-9817-2012, https://www.atmos-chem-phys.net/12/9817/2012/, 2012.

Hwang, H. J. and Ro, C. U.: Direct observation of nitrate and sulfate formations from mineral dust and sea-salts using low-Z particle electron probe X-ray microanalysis, Atmospheric Environment, 40, 3869–3880, https://doi.org/10.1016/j.atmosenv.2006.02.022, 2006.

Jeong, G. Y. and Chun, Y.: Nanofiber calcite in Asian dust and its atmospheric roles, Geophysical Research Letters, 33, 1–5, https://doi.org/10.1029/2006GL028280, 2006.

Jeong, G. Y. and Nousiainen, T.: TEM analysis of the internal structures and mineralogy of Asian dust particles and the implications for optical modeling, Atmospheric Chemistry and Physics, 14, 7233–7254, https://doi.org/10.5194/acp-14-7233-2014, 2014.

Jeong, G. Y., Park, M. Y., Kandler, K., Nousiainen, T., and Kemppinen, O.: Mineralogical properties and internal structures of individual fine particles of Saharan dust, Atmospheric Chemistry and Physics, 16, 12 397–12 410, https://doi.org/10.5194/acp-16-12397-2016, http://www.atmos-chem-phys-discuss.net/acp-2016-308/, 2016.

Jickells, T. D., An, Z. S., Andersen, K. K., Baker, A. R., Bergametti, C., Brooks, N., Cao, J. J., Boyd, P. W., Duce, R. A., Hunter, K. A., Kawahata, H., Kubilay, N., LaRoche, J., Liss, P. S., Mahowald, N., Prospero, J. M., Ridgwell, A. J., Tegen, I., and Torres, R.: Global iron connections between desert dust, ocean biogeochemistry, and climate, Science, 308, 67–71, https://doi.org/10.1126/science.1105959, http://www.sciencemag.org/cgi/doi/10.1126/science.1105959, 2005.

Journet, E., Balkanski, Y., and Harrison, S. P.: A new data set of soil mineralogy for dust-cycle modeling, Atmospheric Chemistry and Physics, 14, 3801–3816, https://doi.org/10.5194/acp-14-3801-2014, http://www.atmos-chem-phys.net/14/3801/2014/, 2014.

Kandler, K., Benker, N., Bundke, U., Cuevas, E., Ebert, M., Knippertz, P., Rodríguez, S., Schütz, L., and Weinbruch, S.: Chemical composition and complex refractive index of Saharan Mineral Dust at Izaña, Tenerife (Spain) derived by electron microscopy, Atmospheric Environment, 41, 8058–8074, https://doi.org/10.1016/j.atmosenv.2007.06.047, 2007.

Kandler, K., Schütz, L., Deutscher, C., Ebert, M., Hofmann, H., Jäckel, S., Jaenicke, R., Knippertz, P., Lieke, K., Massling, A., Petzold, A., Schladitz, A., Weinzierl, B., Wiedensohler, A., Zorn, S., and Weinbruch, S.: Size distribution, mass concentration, chemical and mineralogical composition and derived optical parameters of the boundary layer aerosol at Tinfou, Morocco, during SAMUM 2006, Tellus B, 61, 32–50, https://doi.org/10.1111/j.1600-0889.2008.00385.x, http://www.tellusb.net/index.php/tellusb/article/view/16798, 2009.

Kandler, K., Lieke, K., Benker, N., Emmel, C., Küpper, M., Müller-Ebert, D., Ebert, M., Scheuvens, D., Schladitz, A., Schütz, L., and Weinbruch, S.: Electron microscopy of particles collected at Praia, Cape Verde, during the Saharan Mineral Dust Experiment: particle chemistry, shape, mixing state and complex refractive index, Tellus, Series B: Chemical and Physical Meteorology, 63, 475–496, https://doi.org/10.1111/j.1600-0889.2011.00550.x, 2011a.

Kandler, K., Schütz, L., Jackel, S., Lieke, K., Emmel, C., Müller-Ebert, D., Ebert, M., Scheuvens, D., Schladitz, A., Šegvic, B., Wiedensohler, A., and Weinbruch, S.: Ground-based off-line aerosol measurements at Praia, Cape Verde, during the Saharan Mineral Dust Experiment: Microphysical properties and mineralogy, Tellus, Series B: Chemical and Physical Meteorology, 63, 459–474, https://doi.org/10.1111/j.1600-0889.2011.00546.x, 2011b.

Kaufman, Y. J., Koren, I., Remer, L. A., Tanré, D., Ginoux, P., and Fan, S.: Dust transport and deposition observed from the Terra-Moderate Resolution Imaging Spectroradiometer (MODIS) spacecraft over the Atlantic Ocean, Journal of Geophysical Research D: Atmospheres, 110, 1–16, https://doi.org/10.1029/2003JD004436, 2005.

Kemppinen, O., Nousiainen, T., and Jeong, G. Y.: Effects of dust particle internal structure on light scattering, Atmospheric Chemistry and Physics, 15, 12 011–12 027, https://doi.org/10.5194/acp-15-12011-2015, 2015.

Kim, J.-S. and Park, K.: Atmospheric Aging of Asian Dust Particles During Long Range Transport, Aerosol Science and Technology, 46, 913–924, https://doi.org/10.1080/02786826.2012.680984, 2012.

Knippertz, P. and Todd, M. C.: Mineral dust aerosols over the Sahara: Meteorological controls on emission and transport and implications for modeling, Reviews of Geophysics, 50, https://doi.org/10.1029/2011RG000362, 2012.

Knippertz, P., Deutscher, C., Kandler, K., Müller, T., Schulz, O., and Schütz, L.: Dust mobilization due to density currents in the Atlas region: Observations from the Saharan Mineral Dust Experiment 2006 field campaign, Journal of Geophysical Research Atmospheres, 112, 1–14, https://doi.org/10.1029/2007JD008774, 2007.

Kok, J. F., Ward, D. S., Mahowald, N. M., and Evan, A. T.: Global and regional importance of the direct dust-climate feedback, Nature Communications, 9, https://doi.org/10.1038/s41467-017-02620-y, http://dx.doi.org/10.1038/s41467-017-02620-y, 2018.

Krueger, B. J., Grassian, V. H., Cowin, J. P., and Laskin, A.: Heterogeneous chemistry of individual mineral dust particles from different dust source regions: The importance of particle mineralogy, Atmospheric Environment, 38, 6253–6261, https://doi.org/10.1016/j.atmosenv.2004.07.010, 2004.

Laskin, A., Iedema, M. J., Ichkovich, A., Graber, E. R., Taraniuk, I., and Rudich, Y.: Direct observation of completely processed calcium carbonate dust particles., Faraday discussions, 130, 453–468, https://doi.org/10.1039/b417366j, http://xlink.rsc.org/?DOI=b417366j, 2005.

Liu, D., Taylor, J. W., Crosier, J., Marsden, N., Bower, K. N., Lloyd, G., Ryder, C. L., Brooke, J. K., Cotton, R., Marenco, F., Blyth, A., Cui, Z., Estelles, V., Gallagher, M., Coe, H., and Choularton, T. W.: Aircraft and ground measurements of dust aerosols over the west African coast in summer 2015 during ICE-D and AER-D, Atmospheric Chemistry and Physics, 18, 3817–3838, https://doi.org/10.5194/acp-18-3817-2018, https://www.atmos-chem-phys-discuss.net/acp-2017-984/, 2018.

Marsden, N., Flynn, M. J., Taylor, J. W., Allan, J. D., and Coe, H.: Evaluating the influence of laser wavelength and detection stage geometry on optical detection efficiency in a single-particle mass spectrometer, Atmospheric Measurement Techniques, 9, 6051–6068, https://doi.org/10.5194/amt-9-6051-2016, http://www.atmos-meas-tech-discuss.net/amt-2016-150/, 2016.

Marsden, N. A., Flynn, M. J., Allan, J. D., and Coe, H.: Online differentiation of mineral phase in aerosol particles by ion formation mechanism using a LAAP-TOF single-particle mass spectrometer, Atmospheric Measurement Techniques, 11, 195–213, https://doi.org/10.5194/amt-11-195-2018, 2018.

Matsuki, A., Iwasaka, Y., Shi, G., Zhang, D., Trochkine, D., Yamada, M., Yoon-Suk, K., Chen, B., Nagatani, T., Miyazawa, T., Nagatani, M., and Nakata, H.: Morphological and chemical modification of mineral dust: Observational insight into the heterogeneous uptake of acidic gases, Geophysical Research Letters, 32, 1–4, https://doi.org/10.1029/2005GL024176, 2005.

Möhler, O., Benz, S., Saathoff, H., Schnaiter, M., Wagner, R., Schneider, J., Walter, S., Ebert, V., and Wagner, S.: The effect of organic coating on the heterogeneous ice nucleation efficiency of mineral dust aerosols, Environmental Research Letters, 3, 025 007, https://doi.org/10.1088/1748-9326/3/2/025007, http://stacks.iop.org/1748-9326/3/i=2/a=025007?key=crossref.d9430010506fa5292539821f7ee92ca3, 2008.

Moreno, T., Querol, X., Castillo, S., Alastuey, A., Cuevas, E., Herrmann, L., Mounkaila, M., Elvira, J., and Gibbons, W.: Geochemical variations in aeolian mineral particles from the Sahara-Sahel Dust Corridor, Chemosphere, 65, 261–270, https://doi.org/10.1016/j.chemosphere.2006.02.052, http://www.ncbi.nlm.nih.gov/pubmed/16600327, 2006.

Murphy, D. M.: The design of single particle laser mass spectrometers, Mass Spectrometry Reviews, 26, 150–165, https://doi.org/10.1002/mas, 2007.

Nickovic, S., Vukovic, A., Vujadinovic, M., Djurdjevic, V., and Pejanovic, G.: Technical Note: High-resolution mineralogical database of dust-productive soils for atmospheric dust modeling, Atmospheric Chemistry and Physics, 12, 845–855, https://doi.org/10.5194/acp-12-845-2012, http://www.atmos-chem-phys.net/12/845/2012/acp-12-845-2012.html, 2012.

Niedermeier, D., Shaw, R. a., Hartmann, S., Wex, H., Clauss, T., Voigtländer, J., and Stratmann, F.: Heterogeneous ice nucleation: exploring the transition from stochastic to singular freezing behavior, Atmospheric Chemistry and Physics, 11, 8767–8775, https://doi.org/10.5194/acp-11-8767-2011, http://www.atmos-chem-phys.net/11/8767/2011/, 2011.

Nousiainen, T., Zubko, E., Niemi, J. V., Kupiainen, K., Lehtinen, M., Muinonen, K., and Videen, G.: Single-scattering modeling of thin, birefringent mineral-dust flakes using the discrete-dipole approximation, Journal of Geophysical Research Atmospheres, 114, 1–12, https://doi.org/10.1029/2008JD011564, 2009.

O'Sullivan, D., Murray, B. J., Ross, J. F., and Webb, M. E.: The adsorption of fungal ice-nucleating proteins on mineral dusts: A terrestrial reservoir of atmospheric ice-nucleating particles, Atmospheric Chemistry and Physics, 16, 7879–7887, https://doi.org/10.5194/acp-16-7879-2016, 2016.

Patey, M. D., Achterberg, E. P., Rijkenberg, M. J., and Pearce, R.: Aerosol time-series measurements over the tropical Northeast Atlantic Ocean: Dust sources, elemental composition and mineralogy, Marine Chemistry, 174, 103–119, https://doi.org/10.1016/j.marchem.2015.06.004, http://www.sciencedirect.com/science/article/pii/S030442031500119X, 2015.

Pawlowsky-Glahn, V. and Egozcue, J. J.: Compositional data and their analysis: an introduction, Geological Society, London, Special Publications, 264, 1–10, https://doi.org/10.1144/GSL.SP.2006.264.01.01, http://sp.lyellcollection.org/lookup/doi/10.1144/GSL.SP.2006.264.01.01, 2006.

Peckhaus, A., Kiselev, A., Hiron, T., Ebert, M., and Leisner, T.: A comparative study of K-rich and Na/Ca-rich feldspar ice-nucleating particles in a nanoliter droplet freezing assay, Atmospheric Chemistry and Physics, 16, 11 477–11 496, https://doi.org/10.5194/acp-16-11477-2016, 2016.

Perlwitz, J. P., Pérez García-Pando, C., and Miller, R. L.: Predicting the mineral composition of dust aerosols – Part 1: Representing key processes, Atmospheric Chemistry and Physics, 15, 3493–3575, https://doi.org/10.5194/acpd-15-3493-2015, http://www.atmos-chem-phys-discuss.net/15/3493/2015/, 2015a.

Perlwitz, J. P., Pérez García-Pando, C., and Miller, R. L.: Predicting the mineral composition of dust aerosols - Part 2: Model evaluation and identification of key processes with observations, Atmospheric Chemistry and Physics, 15, 11 629–11 652, https://doi.org/10.5194/acp-15-11629-2015, 2015b.

Pratt, K. a., DeMott, P. J., French, J. R., Wang, Z., Westphal, D. L., Heymsfield, A. J., Twohy, C. H., Prenni, A. J., and Prather, K. a.: In situ detection of biological particles in cloud ice-crystals, Nature Geoscience, 2, 398–401, https://doi.org/10.1038/ngeo521, http://www.nature.com/doifinder/10.1038/ngeo521, 2009.

Price, H. C., Baustian, K. J., McQuaid, J. B., Blyth, A., Bower, K. N., Choularton, T., Cotton, R. J., Cui, Z., Field, P. R., Gallagher, M., Hawker, R., Merrington, A., Miltenberger, A., Neely, R. R., Parker, S. T., Rosenberg, P. D., Taylor, J. W., Trembath, J., Vergara-Temprado, J., Whale, T. F., Wilson, T. W., Young, G., and Murray, B. J.: Atmospheric Ice-Nucleating Particles in the Dusty Tropical Atlantic, Journal of Geophysical Research: Atmospheres, 123, 2175–2193, https://doi.org/10.1002/2017JD027560, 2018.

Rebotier, T. P. and Prather, K. a.: Aerosol time-of-flight mass spectrometry data analysis: a benchmark of clustering algorithms., Analytica chimica acta, 585, 38–54, https://doi.org/10.1016/j.aca.2006.12.009, http://www.ncbi.nlm.nih.gov/pubmed/17386645, 2007.

Reilly, P. T. a., Lazar, a. C., Gieray, R. a., Whitten, W. B., and Ramsey, J. M.: The Elucidation of Charge-Transfer-Induced Matrix Effects in Environmental Aerosols Via Real-Time Aerosol Mass Spectral Analysis of Individual Airborne Particles, Aerosol Science and Technology, 33, 135–152, https://doi.org/10.1080/027868200410895, http://www.tandfonline.com/doi/abs/10.1080/027868200410895, 2000.

Reinard, M. S. and Johnston, M. V.: Ion formation mechanism in laser desorption ionization of individual nanoparticles., Journal of the American Society for Mass Spectrometry, 19, 389–99, https://doi.org/10.1016/j.jasms.2007.11.017, http://www.ncbi.nlm.nih.gov/pubmed/18191579, 2008.

Reitz, P., Spindler, C., Mentel, T. F., Poulain, L., Wex, H., Mildenberger, K., Niedermeier, D., Hartmann, S., Clauss, T., Stratmann, F., Sullivan, R. C., DeMott, P. J., Petters, M. D., Sierau, B., and Schneider, J.: Surface modification of mineral dust particles by sulphuric acid processing: implications for ice nucleation abilities, Atmospheric Chemistry and Physics, 11, 7839–7858, https://doi.org/10.5194/acp-11-7839-2011, http://www.atmos-chem-phys.net/11/7839/2011/, 2011.

Ro, C. U., Hwang, H., Kim, H., Chun, Y., and Van Grieken, R.: Single-particle characterization of four "Asian Dust" samples collected in Korea, using low-Z particle electron probe X-ray microanalysis, Environmental Science and Technology, 39, 1409–1419, https://doi.org/10.1021/es049772b, 2005.

Rosenfeld, D., Rudich, Y., and Lahav, R.: Desert dust suppressing precipitation: a possible desertification feedback loop., Proceedings of the National Academy of Sciences of the United States of America, 98, 5975–80, https://doi.org/10.1073/pnas.101122798, http://www.pnas.org.proxy.library.uu.nl/content/98/11/5975.short, 2001.

Ryder, C. L., Highwood, E. J., Lai, T. M., Sodemann, H., and Marsham, J. H.: Impact of atmospheric transport on the evolution of microphysical and optical properties of Saharan dust, Geophysical Research Letters, 40, 2433–2438, https://doi.org/10.1002/grl.50482, 2013.

Salvador, P., Almeida, S. M., Cardoso, J., Almeida-Silva, M., Nunes, T., Cerqueira, M., Alves, C., Reis, M. A., Chaves, P. C., Artíñano, B., and Pio, C.: Composition and origin of PM10 in Cape Verde: Characterization of long-range transport episodes, Atmospheric Environment, 127, 326–339, https://doi.org/10.1016/j.atmosenv.2015.12.057, 2016.

Scanza, R. A., Mahowald, N., Ghan, S., Zender, C. S., Kok, J. F., Liu, X., Zhang, Y., and Albani, S.: Modeling dust as component minerals in the Community Atmosphere Model: Development of framework and impact on radiative forcing, Atmospheric Chemistry and Physics, 15, 537–561, https://doi.org/10.5194/acp-15-537-2015, 2015.

Schepanski, K., Tegen, I., and MacKe, A.: Saharan dust transport and deposition towards the tropicalnorthern Atlantic, Atmospheric Chemistry and Physics, 9, 1173–1189, https://doi.org/10.5194/acp-9-1173-2009, 2009a.

Schepanski, K., Tegen, I., Todd, M. C., Heinold, B., Bönisch, G., Laurent, B., and Macke, A.: Meteorological processes forcing Saharan dust emission inferred from MSG-SEVIRI observations of subdaily dust source activation and numerical models, Journal of Geophysical Research Atmospheres, 114, 1–18, https://doi.org/10.1029/2008JD010325, 2009b.

Schepanski, K., Tegen, I., and Macke, A.: Comparison of satellite based observations of Saharan dust source areas, Remote Sensing of Environment, 123, 90–97, https://doi.org/10.1016/j.rse.2012.03.019, http://dx.doi.org/10.1016/j.rse.2012.03.019, 2012.

Scheuvens, D., Schütz, L., Kandler, K., Ebert, M., and Weinbruch, S.: Bulk composition of northern African dust and its source sediments - A compilation, Earth-Science Reviews, 116, 170–194, https://doi.org/10.1016/j.earscirev.2012.08.005, http://dx.doi.org/10.1016/j.earscirev.2012.08.005, 2013.

Schmidt, S., Schneider, J., Klimach, T., Mertes, S., Schenk, L. P., Kupiszewski, P., Curtius, J., and Borrmann, S.: Online single particle analysis of ice particle residuals from mountain-top mixed-phase clouds using laboratory derived particle type assignment, Atmospheric Chemistry and Physics, 17, 575–594, https://doi.org/10.5194/acp-17-575-2017, http://www.atmos-chem-phys-discuss.net/acp-2016-365/, 2017.

Shen, X., Ramisetty, R., Mohr, C., Huang, W., Leisner, T., and Saathoff, H.: Laser ablation aerosol particle time-of-flight mass spectrometer (LAAPTOF): Performance, reference spectra and classification of atmospheric samples, Atmospheric Measurement Techniques, 11, 2325–2343, https://doi.org/10.5194/amt-11-2325-2018, https://www.atmos-meas-tech-discuss.net/amt-2017-338/amt-2017-338.pdf, 2018.

Silva, P. and Prather, K.: Interpretation of mass spectra from organic compounds in aerosol time-of-flight mass spectrometry, Analytical chemistry, 72, 3553–62, http://www.ncbi.nlm.nih.gov/pubmed/10952542, 2000.

Sobanska, S., Hwang, H., Choël, M., Jung, H. J., Eom, H. J., Kim, H., Barbillat, J., and Ro, C. U.: Investigation of the chemical mixing state of individual asian dust particles by the combined use of electron probe X-ray microanalysis and raman microspectrometry, Analytical Chemistry, 84, 3145–3154, https://doi.org/10.1021/ac2029584, 2012.

Sodeman, D. A., Toner, S. M., and Prather, K. A.: Determination of single particle mass spectral signatures from light-duty vehicle emissions, Environmental Science and Technology, 39, 4569–4580, https://doi.org/10.1021/es0489947, 2005.

Sullivan, R. C. and Prather, K. a.: Recent advances in our understanding of atmospheric chemistry and climate made possible by on-line aerosol analysis instrumentation., Analytical chemistry, 77, 3861–85, https://doi.org/10.1021/ac050716i, http://www.ncbi.nlm.nih.gov/pubmed/15952760, 2005.

Sullivan, R. C., Guazzotti, S. A., Sodeman, D. A., and Prather, K. a.: Direct observations of the atmospheric processing of Asian mineral dust, Atmospheric Chemistry and Physics, 7, 1213–1236, https://doi.org/10.5194/acp-7-1213- 2007, 2007a.

Sullivan, R. C., Guazzotti, S. a., Sodeman, D. a., Tang, Y., Carmichael, G. R., and Prather, K. a.: Mineral dust is a sink for chlorine in the marine boundary layer, Atmospheric Environment, 41, 7166–7179, https://doi.org/10.1016/j.atmosenv.2007.05.047, 2007b.

Sullivan, R. C., Miñambres, L., Demott, P. J., Prenni, A. J., Carrico, C. M., Levin, E. J. T., and Kreidenweis, S. M.: Chemical processing does not always impair heterogeneous ice nucleation of mineral dust particles, Geophysical Research Letters, 37, 1–5, https://doi.org/10.1029/2010GL045540, 2010a.

Sullivan, R. C., Petters, M. D., Demott, P. J., Kreidenweis, S. M., Wex, H., Niedermeier, D., Hartmann, S., Clauss, T., Stratmann, F., Reitz, P., Schneider, J., and Sierau, B.: Irreversible loss of ice nucleation active sites in mineral dust particles caused by sulphuric acid condensation, Atmospheric Chemistry and Physics, 10, 11 471–11 487, https://doi.org/10.5194/acp-10-11471-2010, 2010b.

Tobo, Y., Zhang, D. Z., Nakata, N., Yamada, M., Ogata, H., Hara, K., and Iwasaka, Y.: Hygroscopic mineral dust particles as influenced by chlorine chemistry in the marine atmosphere, Geophysical Research Letters, 36, L05 817, https://doi.org/10.1029/2008GL036883, 2009.

Tsamalis, C., Chédin, A., Pelon, J., and Capelle, V.: The seasonal vertical distribution of the saharan air layer and its modulation by the wind, Atmospheric Chemistry and Physics, 13, 11 235–11 257, https://doi.org/10.5194/acp-13-11235-2013, 2013.

Usher, C. R., Michel, A. E., and Grassian, V. H.: Reactions on mineral dust., Chemical reviews, 103, 4883–4939, https://doi.org/10.1021/cr020657y, http://www.ncbi.nlm.nih.gov/pubmed/14664636, 2003.

Wonaschuetz, A., Kallinger, P., Szymanski, W., and Hitzenberger, R.: Chemical composition of radiolytically formed particles using single-particle mass spectrometry, Journal of Aerosol Science, 113, 242–249, https://doi.org/10.1016/j.jaerosci.2017.07.012, http://dx.doi.org/10.1016/j.jaerosci.2017.07.012, 2017.

Worringen, A., Kandler, K., Benker, N., Dirsch, T., Mertes, S., Schenk, L., Kastner, U., Frank, F., Nillius, B., Bundke, U., Rose, D., Curtius, J., Kupiszewski, P., Weingartner, E., Vochezer, P., Schneider, J., Schmidt, S., Weinbruch, S., and Ebert, M.: Single-particle characterization of ice-nucleating particles and ice particle residuals sampled by three different techniques, Atmospheric Chemistry and Physics, 15, 4161–4178, https://doi.org/10.5194/acp-15-4161-2015, 2015.

Yamaguchi, N., Ichijo, T., Sakotani, A., Baba, T., and Nasu, M.: Global dispersion of bacterial cells on Asian dust., Scientific reports, 2, 525, https://doi.org/10.1038/srep00525, http://www.pubmedcentral.nih.gov/articlerender.fcgi?artid=3401963&tool=pmcentrez&rendertype=abstract, 2012.

Young, G., Jones, H. M., Darbyshire, E., Baustian, K. J., McQuaid, J. B., Bower, K. N., Connolly, P. J., Gallagher, M. W., and Choularton, T. W.: Size-segregated compositional analysis of aerosol particles collected in the European Arctic during the ACCACIA campaign, Atmospheric Chemistry and Physics, 16, 4063–4079, https://doi.org/10.5194/acp-16-4063-2016, 2016.

Yuan, H., Rahn, K. A., and Zhuang, G.: Graphical techniques for interpreting the composition of individual aerosol particles, Atmospheric Environment, 38, 6845–6854, https://doi.org/10.1016/j.atmosenv.2004.09.010, 2004.

Zawadowicz, M. A., Froyd, K. D., Murphy, D. M., and Cziczo, D. J.: Improved identification of primary biological aerosol particles using single-particle mass spectrometry, Atmospheric Chemistry and Physics, 17, 7193–7212, https://doi.org/10.5194/acp-17-7193-2017, http://www.atmos-chem-phys-discuss.net/acp-2016-1119/, 2017.

Zelenyuk, A., Yang, J., Choi, E., and Imre, D.: SPLAT II: An Aircraft Compatible, Ultra-Sensitive, High Precision Instrument for In-Situ Characterization of the Size and Composition of Fine and Ultrafine Particles, Aerosol Science and Technology, 43, 411–424, https://doi.org/10.1080/02786820802709243, http://www.tandfonline.com/doi/abs/10.1080/02786820802709243, 2009.

Zelenyuk, A., Imre, D., Wilson, J., Zhang, Z., Wang, J., and Mueller, K.: Airborne Single Particle Mass Spectrometers (SPLAT II & min-iSPLAT) and New Software for Data Visualization and Analysis in a Geo-Spatial Context., Journal of the American Society for Mass Spectrometry, https://doi.org/10.1007/s13361-014-1043-4, http://www.ncbi.nlm.nih.gov/pubmed/25563475, 2015.

Zhu, A., Ramanathan, V., Li, F., and Kim, D.: Dust plumes over the Pacific, Indian, and Atlantic oceans: Climatology and radiative impact, Journal of Geophysical Research Atmospheres, 112, 1–20, https://doi.org/10.1029/2007JD008427, 2007.

Zimmermann, F., Weinbruch, S., Schütz, L., Hofmann, H., Ebert, M., Kandler, K., and Worringen, A.: Ice nucleation properties of the most abundant mineral dust phases, Journal of Geophysical Research Atmospheres, 113, https://doi.org/10.1029/2008JD010655, 2008.